C.93
G6R

TECHNOLOGY

Journal of Research

of the

National Bureau of Standards

PUBLIC LIBRARY
APR 21 1959
DETROIT

MARCH 1959

VOLUME 62 NUMBER 3

U. S. DEPARTMENT OF COMMERCE
Lewis L. Strauss, Secretary
NATIONAL BUREAU OF STANDARDS
A. V. Astin, Director

MARCH • 1959
VOLUME • 62
NUMBER • 3

JOURNAL OF RESEARCH

of the

NATIONAL BUREAU OF STANDARDS

The National Bureau of Standards

Functions and Activities

The functions of the National Bureau of Standards are set forth in the Act of Congress, March 3, 1901, as amended by Congress in Public Law 619, 1950. These include the development and maintenance of the national standards of measurement and the provision of means and methods for making measurements consistent with these standards; the determination of physical constants and properties of materials; the development of methods and instruments for testing materials, devices, and structures; advisory services to government agencies on scientific and technical problems; invention and development of devices to serve special needs of the Government; and the development of standard practices, codes, and specifications. The work includes basic and applied research, development, engineering, instrumentation, testing, evaluation, calibration services, and various consultation and information services. Research projects are also performed for other government agencies when the work relates to and supplements the basic program of the Bureau or when the Bureau's unique competence is required. The scope of activities is suggested by the listing of divisions and sections on the inside of the back cover.

Publications

The results of the Bureau's work take the form of either actual equipment and devices or published papers. These papers appear either in the Bureau's own series of publications or in the journals of professional and scientific societies. The Bureau itself publishes three monthly periodicals, available from the Government Printing Office: The Journal of Research, which presents complete papers reporting technical investigations; the Technical News Bulletin, which presents summary and preliminary reports on work in progress; and Basic Radio Propagation Predictions, which provides data for determining the best frequencies to use for radio communications throughout the world. There are also five series of nonperiodical publications: The Applied Mathematics Series, Circulars, Handbooks, Building Materials and Structures Reports, and Miscellaneous Publications.

Information on the Bureau's publications can be found in NBS Circular 460, Publications of the National Bureau of Standards ($1.25) and its Supplement ($1.50), available from the Superintendent of Documents, Government Printing Office, Washington 25, D.C.

Order all publications from the Superintendent of Documents
U.S. Government Printing Office, Washington 25, D.C.

Use of funds for printing this publication approved by the Director of the Bureau of the Budget (June 24, 1958)

Journal of Research of the National Bureau of Standards Vol. 62, No. 3, March 1959 Research Paper 2935

On a Theorem of M. Riesz[1]

Martin Pearl[2]

The structure of the set of skew-symmetric, orthogonal matrices of order 4 with elements in the real field is studied. The first and second regular representations of the quaternions are used to represent these matrices and known properties of the quaternions are exploited to obtain characterizations of the skew-symmetric matrices. In the second part of this paper, the underlying structure of the geometry is changed from the Euclidean to the Lorentzian. It is then shown that there are no skew-symmetric, orthogonal (in the Lorentzian sense) matrices of order 4.

1. Introduction

In a series of lectures [6][3] recently delivered at the University of Maryland (Sept. 1957 to Feb. 1958) dealing with Clifford algebras, M. Riesz proved the following

THEOREM. *If A and B are real skew-symmetric, orthogonal linear transformations on E_4 (a real four-dimensional vector space on which there is imposed a Euclidean metric), then $[A, B]=AB-BA$ is a multiple of a real skew-symmetric, orthogonal transformation on E_4.*

The main purpose of this paper is to exhibit a proof of this theorem which does not depend on the structure of the Clifford algebra, but only on the properties of the matrices associated with these transformations. Moreover, it will be shown that if the underlying geometry is changed from the Euclidean metric to the Lorentzian metric, then the theorem is vacuously true since no real skew-symmetric, orthogonal (in the Lorentzian sense) matrices of order 4 exist. The main tools used herein are real quaternions and their representations by 4×4 matrices. Incidentally, a method is given for constructing all skew-symmetric orthogonal matrices of order 4.

2. Regular Representations

Let $\mathfrak{A}$ be an algebra over the (commutative) field $\mathfrak{F}$ and let $e_1, e_2, \ldots, e_n$ be a basis of $\mathfrak{A}$. Multiplication of two elements in A is completely determined by the multiplication of the basal elements. Since $e_1, e_2, \ldots, e_n$ forms a basis for $\mathfrak{A}$,

$$e_i e_j=\sum_{k=1}^{n} c_{ijk}e_k \qquad c_{ijk}\epsilon\mathfrak{F}, \tag{1}$$

and it is well known that associativity in $\mathfrak{A}$ is equivalent to the n^4 equations.

$$\sum_{k=1}^{n} c_{ijk}c_{klm}=\sum_{k=1}^{n} c_{ikm}c_{jlk} \qquad (i, j, l, m=1, 2, \ldots, n). \tag{2}$$

---

[1] This work was completed while the author held a National Research Council-National Bureau of Standards Postdoctoral Research Associateship at the National Bureau of Standards, Washington, D. C.

[2] Present address: University of Maryland, College Park, Maryland.

[3] Figures in brackets indicate the literature references at the end of this paper.

If we define the $n\times n$ matrices $R_i=(c_{isr})$ and $S_i=(c_{rts})$ (where r denotes the row index and s denotes the column index), then, by successively setting (i) $m=r$, $l=s$; (ii) $i=r$, $m=s$; and (iii) $j=r$, $m=s$, we have

$$\text{(i)}\ R_iR_j=\sum_{k=1}^{n}c_{ijk}R_k \qquad \text{(ii)}\ S_iS_j=\sum_{k=1}^{n}c_{ijk}S_k \tag{3}$$

and

$$\text{(iii)}\ R_i'S_j=S_jR_i', \tag{4}$$

where R_i' is the transpose of R_i.

Every element a of $\mathfrak{A}$ can be written uniquely in the form

$$a=\alpha_1e_1+\alpha_2e_2+\ \ldots\ +\alpha_ne_n \qquad \alpha_i\epsilon\mathfrak{F}. \tag{5}$$

If we define

$$R(a)=\alpha_1R_1+\alpha_2R_2+\ \ldots\ +\alpha_nR_n,\ S(a)=\alpha_1S_1+\alpha_2S_2+\ \ldots\ +\alpha_nS_n \tag{6}$$

then the mappings $a\to R(a)$ and $a\to S(a)$ of $\mathfrak{A}$ into the algebras of matrices, $\mathfrak{R}$ and $\mathfrak{S}$, are homomorphisms, called *the first and second regular representations* of $\mathfrak{A}$. If we further assume that $\mathfrak{A}$ has an identity, then these mappings are isomorphisms.

We shall be interested in the particular case where $\mathfrak{A}$ is the algebra $\mathfrak{Q}$ of real quaternions, that is, the algebra over the real field with basis elements e_0, e_1, e_2, e_3 satisfying the following conditions:

$$\begin{aligned}&\text{(i)}\quad e_0 \text{ is the identity element of } \mathfrak{Q},\\ &\text{(ii)}\quad e_1e_2=-e_2e_1=e_3,\ e_2e_3=-e_3e_2=e_1,\ e_3e_1=-e_1e_3=e_2,\\ &\text{(iii)}\quad e_1^2=e_2^2=e_3^2=-e_0.\end{aligned} \tag{7}$$

Then $R_0=S_0=I$ (the identity matrix) and

$$R_1=\begin{bmatrix}0&-1&0&0\\1&0&0&0\\0&0&0&-1\\0&0&1&0\end{bmatrix}\quad R_2=\begin{bmatrix}0&0&-1&0\\0&0&0&1\\1&0&0&0\\0&-1&0&0\end{bmatrix}\quad R_3=\begin{bmatrix}0&0&0&-1\\0&0&-1&0\\0&1&0&0\\1&0&0&0\end{bmatrix}. \tag{8}$$

$$S_1=\begin{bmatrix}0&1&0&0\\-1&0&0&0\\0&0&0&-1\\0&0&1&0\end{bmatrix}\quad S_2=\begin{bmatrix}0&0&1&0\\0&0&0&1\\-1&0&0&0\\0&-1&0&0\end{bmatrix}\quad S_3=\begin{bmatrix}0&0&0&1\\0&0&-1&0\\0&1&0&0\\-1&0&0&0\end{bmatrix}. \tag{9}$$

Clearly, R_1, R_2, R_3, S_1, S_2, S_3 are each skew-symmetric and hence $\mathfrak{Q}_0$, the additive group of all linear combinations of the R's and S's with real coefficients, is contained in $\mathfrak{Q}_1$, the additive group of all 4×4 real skew-symmetric matrices. However,

$$\begin{aligned}Q=\begin{bmatrix}0&a&b&c\\-a&0&d&e\\-b&-d&0&f\\-c&-e&-f&0\end{bmatrix}&=\tfrac{1}{2}[a(S_1-R_1)+b(S_2-R_2)+c(S_3-R_3)-d(S_3+R_3)\\&\quad+e(S_2+R_2)-f(S_1+R_1)],\end{aligned} \tag{10}$$

that is, every skew-symmetric matrix Q can be expressed as a linear combination of R_1, R_2, R_3, S_1, S_2, S_3. Thus, $\mathfrak{Q}_1\subseteq\mathfrak{Q}_0$ and hence $\mathfrak{Q}_1=\mathfrak{Q}_0$. Since $\mathfrak{Q}_1$ has dimension six (when considered as a real vector space), it follows that R_1, R_2, R_3, S_1, S_2, S_3 are linearly independent and form a

basis for Q_1. Hence, we have shown that *every* 4×4 ***skew-symmetric matrix*** Q *can be expressed as* $R(a)+S(b)$ *for a unique pair of quaternions,* $a=\alpha_1e_1+\alpha_2e_2+\alpha_3e_3$ and $b=\beta_1e_1+\beta_2e_2+\beta_3e_3$. A quaternion whose e_0-coefficient is zero is called a *pure quaternion*.

3. Skew-Symmetric, Orthogonal Matrices

We are particularly interested in those matrices Q of $\mathfrak{Q}_1$ which are also orthogonal, and we shall be able to characterize them in terms of the pure quaternions a and b.

Since each of the R's and S's is skew-symmetric, (4) may be replaced by

$$R(a)\,S(b)=S(b)\,R(a). \tag{11}$$

We define the *norm*, $N(a)$, of the pure quaternion $a=\alpha_1e_1+\alpha_2e_2+\alpha_3e_3$ to be $\alpha_1^2+\alpha_2^2+\alpha_3^2$. Thus, $N(a)\geq0$ and $N(a)=0$ if and only if $a=0$. Furthermore, $N(\alpha a)=\alpha^2N(a)$ for every real number α. It follows from (7) that $a^2=-N(a)e_0$ and hence

$$R(a)^2=S(a)^2=-N(a)\,I. \tag{12}$$

Furthermore, if $a\neq0$, then $c=a/\sqrt{N(a)}$ has norm 1 and is called the unit quaternion in the direction of a.

We shall now derive some useful properties of the matrices $R(a)$ and $S(a)$ by means of the mapping σ of the real vector $\vec{a}=(\alpha_1,\ \alpha_2,\ \alpha_3)$ into the quaternion $a=\sigma(\vec{a})$. This mapping is clearly an additive isomorphism. Furthermore,

$$\begin{aligned}ab=\sigma(\vec{a})\sigma(\vec{b})&=-(\alpha_1\beta_1+\alpha_2\beta_2+\alpha_3\beta_3)e_0+(\alpha_1\beta_2-\alpha_2\beta_1)e_3\\&\quad+(\alpha_3\beta_1-\alpha_1\beta_3)e_2+(\alpha_2\beta_3-\alpha_3\beta_2)e_1=-(\vec{a}\cdot\vec{b})e_0+\sigma(\vec{a}*\vec{b})\end{aligned} \tag{13}$$

where $\vec{a}\cdot\vec{b}$ is the scalar or dot product of $\vec{a}$ and $\vec{b}$ and $\vec{a}*\vec{b}$ is the vector product of $\vec{a}$ and $\vec{b}$. Since the mappings $a\to R(a)$ and $a\to S(a)$ are isomorphisms, we have

$$R(a)R(b)=-(\vec{a}\cdot\vec{b})I+R[\sigma(\vec{a}*\vec{b})],\qquad S(a)S(b)=-(\vec{a}\cdot\vec{b})I+S[\sigma(\vec{a}*\vec{b})]. \tag{14}$$

It is well known that $\vec{a}*\vec{b}=-\vec{b}*\vec{a}$ and since $\sigma(-a)=-\sigma(a)$, it follows immediately from (14) that

LEMMA 1. *If* a *and* b *are orthogonal pure quaternions (or equivalently, if* $\vec{a}\cdot\vec{b}=0$*), then* $R(a)R(b)=-R(b)R(a)$. *Similarly, if* a *and* b *are orthogonal pure quaternions, then*

$$S(a)S(b)=-S(b)S(a).$$

We define the *conjugate*, $\overline{Q}$, of the skew-symmetric matrix $Q=R(a)+S(b)$ to be $R(a)-S(b)$, and the *norm*, $N(Q)$, of Q to be $N(b)-N(a)$. It follows from (7) and (11) that

$$\begin{aligned}Q\overline{Q}&=[R(a)+S(b)]\,[R(a)-S(b)]=[R(a)]^2-[S(b)]^2=\overline{Q}Q\\&=[-N(a)+N(b)]\,I=N(Q)\,I=N(\overline{Q})\,I.\end{aligned} \tag{15}$$

Now, let $\vec{c}$ be any vector which is orthogonal to $\vec{b}$. Then c is orthogonal to b and it follows from (11) and Lemma 1 that

$$S(c)QS(c)^{-1}=S(c)[R(a)+S(b)]S(c)^{-1}=R(a)-S(b)=\overline{Q}. \tag{16}$$

Thus, Q and $\overline{Q}$ are similar matrices and consequently have the same rank. Furthermore,

$\det(Q)=\det(\overline{Q})$ and by taking the determinants of the terms in (15) we have $\det(Q)\det(\overline{Q})=\det[N(Q)\,I]=N(Q)^4$. Since the determinant of every real skew-symmetric matrix is non-negative, we have proven

LEMMA 2. $\mathrm{Det}\,(Q)=\mathrm{Det}\,(\overline{Q})=N(Q)^2$.

We are now in a position to prove the main theorem of this paper. Riesz' Theorem, stated at the beginning of this paper, follows immediately as a corollary.

THEOREM 1. *The skew-symmetric matrix Q is orthogonal if and only if one of the following conditions is satisfied:*

(i) $N(Q)=-1$ *and* $b=0$, (*and thus* $Q=R(a)$).
(ii) $N(Q)=+1$ *and* $a=0$, (*and thus* $(Q=S(b))$.

PROOF. Let Q be orthogonal. Then $Q^{-1}=-Q$ and since, by (15), $\overline{Q}=N(Q)\;Q^{-1}$, it follows that

$$\overline{Q}=-N(Q)\;Q. \tag{17}$$

Taking the norm of each side of this equation, we have

$$N(Q)=N(\overline{Q})=N[-N(Q)]=[-N(Q)]^2\;N(Q)=[N(Q)]^3. \tag{18}$$

Since Q is nonsingular, $N(Q)\neq 0$ and hence $N(Q)=\pm 1$.

Case 1. $N(Q)=+1$. Substituting this value in (17), we have

$$0=Q+\overline{Q}=[R(a)+S(b)]+[R(a)-S(b)]=2\;R(a). \tag{19}$$

Thus, $R(a)=0$ and hence $a=0$.

Case 2. $N(Q)=-1$. Again, by (17), we have

$$0=Q-\overline{Q}=[R(a)+S(b)]-[R(a)-S(b)]=2\;S(b). \tag{20}$$

As before, $b=0$.

Conversely, if $b=0$ then $Q=\overline{Q}$ and it follows from (15) that if $N(Q)=-1$ then $Q\overline{Q}=Q^2=-I$. Thus Q is orthogonal. Similarly, if $a=0$ then $Q=-\overline{Q}$ and it follows from $N(Q)=+1$ that $Q\overline{Q}=Q^2=-I$. Again, Q is orthogonal.

To prove Riesz' Theorem, let P and Q be two skew-symmetric, orthogonal matrices. Clearly, we can assume that $P=R(a)$ for some pure unit quaternion a. If $Q=S(b)$ for some b, then, by (11), $[P,Q]=PQ-QP=0$. On the other hand, if $Q=R(b)$ for some b, then, using (14), we have

$$[P,\,Q]=R(a)R(b)-R(b)R(a)=2\;R[\sigma(\vec{a}*\vec{b})]=R[\sigma(2(a*b))]. \tag{21}$$

If $\vec{a}=\pm\vec{b}$, then $\vec{a}*\vec{b}=0$ and $[P,\,Q]=0$. If $\vec{a}\neq\pm\vec{b}$, then $\vec{a}*\vec{b}\neq 0$. Since a and b each have norm 1, $N[\sigma(2(\vec{a}*\vec{b}))]=4N[\sigma(\vec{a}*\vec{b})]=4\delta$ where $1\geq\delta>0$. If we now set $\vec{c}=2(\vec{a}*\vec{b})/\sqrt{4\delta}=(\vec{a}*\vec{b})/\sqrt{\delta}$, then $R[\sigma(2(\vec{a}*\vec{b}))]=4\delta R(c)$. Since c is a unit quaternion, $R(c)$ is a skew-symmetric, orthogonal matrix and the theorem is proved.

COROLLARY 1. *Let P, Q be skew-symmetric, orthogonal matrices such that $P\neq\pm Q$. Then P and Q commute if and only if $N(P)N(Q)=-1$.*

COROLLARY 2. *Every skew-symmetric matrix Q can be written as $\alpha R+\beta S$ for unique α, β, R, S, where α, β are real numbers and R, S are skew-symmetric orthogonal matrices.*

4. The Lorentzian Metric

The Lorentzian metric on a real four-dimensional vector space V is defined by the matrix

$$J=\begin{bmatrix} +1 & 0 & 0 & 0 \\ 0 & +1 & 0 & 0 \\ 0 & 0 & +1 & 0 \\ 0 & 0 & 0 & -1 \end{bmatrix}. \tag{22}$$

We shall denote this space by $\mathfrak{L}_4$.

The norm, $N(x)$, of a vector $x=(x_1, x_2, x_3, x_4)$ is given by $x'Jx=x_1^2+x_2^2+x_3^2-x_4^2$. Clearly, $N(x)$ may now take on all real values. If $N(x)=0$, it does not follow that $x=0$. A vector satisfying this equation is said to be isotropic or lightlike. We define a matrix A to be orthogonal with respect to J (or Lorentzian-orthogonal) if $A'JA=J$. An alternate definition for the Lorentzian-orthogonality of a matrix is that it be the matrix of a norm-preserving linear transformation on $\mathfrak{L}_4$.

By analogy with the Euclidean case, we define a matrix Q to be skew-symmetric if it satisfies the equation $x'Qx=0$ for every vector x in $\mathfrak{L}_4$. Then, Q is skew-symmetric in the Lorentzian sense if and only if QJ is skew-symmetric in the Euclidean sense. Furthermore,

LEMMA 3. *A is both orthogonal and skew-symmetric (in the Lorentzian sense) if and only if $A=QJ$ for some skew-symmetric (in the Euclidean sense) matrix Q and*

$$(JQ)^2=(QJ)^2=-I. \tag{23}$$

Thus, we have reduced the problem of Lorentzian skew-symmetric, orthogonal matrices to a corresponding problem involving Euclidean skew-symmetric matrices satisfying (23).

THEOREM 2. *There does not exist a matrix Q satisfying* (23).

PROOF. A simple calculation shows that

$$JR_iJ=\pm S_i, \qquad JS_iJ=\pm R_i, \qquad (+ \text{ when } i=3, - \text{ when } i=1,2). \tag{24}$$

Suppose there exists a skew-symmetric matrix Q satisfying (23). Then we can set $Q=R(a)+S(b)$ for some a and b and $JQJ=R(c)+S(d)$. By (24), $N(c)=N(b)$ and $N(d)=N(a)$. Hence,

$$N(Q)=N(\overline{Q})=-N(JQJ). \tag{25}$$

Since $(QJ)^2=-I$, we have $(\det Q)^2\ (\det J)^2=(\det Q)^2=(\det(-I))=+1$. Combining this with Lemma 2, we have

$$[N(Q)]^2=\det Q=\det \overline{Q}=+1. \tag{26}$$

Also, it follows from (15) that $Q^{-1}=(1/N(Q))\overline{Q}$ and from (23) that $Q^{-1}=-JQJ$. Equating these two expressions and taking the norm of each term yields

$$N(Q)=-N(JQJ)=-N(Q^{-1})=-N[(1/N(Q))\overline{Q}]=-[1/N(Q)]^2\,N(\overline{Q})=-1/N(Q). \tag{27}$$

Thus, $N(Q)^2=-1$, which contradicts (26).

5. Conclusion

The corresponding problem in the two-dimensional case is trivial since there only exist two skew-symmetric orthogonal (Euclidean) matrices, namely, $\begin{bmatrix} 0 & 1 \\ -1 & 0 \end{bmatrix}$ and $\begin{bmatrix} 0 & -1 \\ 1 & 0 \end{bmatrix}$. These clearly commute since one is the negative of the other. On the other hand, if the quadratic

form of the metric is given by $\begin{bmatrix} 1 & 0 \\ 0 & -1 \end{bmatrix}$ then it can be shown that no skew-symmetric Lorentzian, orthogonal matrices exist.

Little is known about the structure of higher dimensional skew-symmetric orthogonal matrices. The methods of this paper are isolated and it is not expected that they can be used in a discussion of higher dimensions.

6. References

[1] H. S. M. Coxeter, Quaternions and reflections. Amer. Math. Monthly **53,** 136 (1946).
[2] L. E. Dickson, Algebras and their arithmetics (Chicago, 1923).
[3] C. C. MacDuffee, Modules and ideals in a Frobenius algebra, Monatsh. Math. und Phys., **48,** 293 (1939).
[4] C. C. MacDuffee, Orthogonal matrices in four-space, Canadian J. Math. **1,** 69–72(1949).
[5] C. C. MacDuffee, The theory of matrices (Chelsea, N. Y., 1946).
[6] M. Riesz, Clifford numbers and the equation of Dirac (Lectures, Univ. of Maryland, 1957–8, unpublished)

Washington, August 21, 1958.

Journal of Research of the National Bureau of Standards Vol. 62, No. 3, March 1959 Research Paper 2936

Refinement of the Crystal Structure of Triclinic Magnesium Pyroborate

Stanley Block, Gordon Burley, Alvin Perloff, and Robert D. Mason, Jr.

The triclinic modification of $Mg_2B_2O_5$ was classified as a member of an isostructural series which also includes $Mn_2B_2O_5$, $Fe_2B_2O_5$, and $Co_2B_2O_5$. The crystal structure was refined by the use of successive Fourier projections and a least-squares refinement program on an electronic computer. The structure of $Mg_2B_2O_5$ consists of $B_2O_5^{-4}$ groups and Mg^{+2} ions. Each magnesium atom is surrounded octahedrally by six oxygen atoms, forming an extended sheet of octahedra. The pyroborate groups share corners with octahedra in the sheets and thus link them. Each boron atom is in planar triangular coordination with three oxygen atoms. The pyroborate group has two such triangles with one shared oxygen. The angle between the planes formed by the triangles is 16°. The average boron-to-oxygen distance is 1.38 A.

1. Introduction

As part of an over-all study of the crystal chemistry of borates it was decided to study the crystal structure of magnesium borate. The American Society for Testing Materials file [1] [1] indicates that MgB_2O_4 is isomorphous with the corresponding manganous and ferrous compounds. This series would be an excellent choice for study because the Mn or Fe could be used to determine the approximate structure by heavy atom techniques. The Mg compound would then be used to determine the bond distances and angles accurately.

Single crystal work on the magnesium compound was undertaken and the cell constants were determined. These indicated that the magnesium compound is isomorphous with $2CoO{\cdot}B_2O_3$ [2]. In addition, the phase diagram of the system MgO-B_2O_3 [3] shows that the solid crystallizing from a melt of composition $MgO{\cdot}B_2O_3$ will have the composition $2MgO{\cdot}B_2O_3$ since $MgO{\cdot}B_2O_3$ does not exist in equilibrium with the liquid. A monoclinic phase and a triclinic phase of manganous pyroborate were found. The ferrous pyroborate and the triclinic phase of manganous pyroborate were also proven isomorphous with the cobalt and magnesium pyroborates, so that the correct formula for the series is not MB_2O_4 but $M_2B_2O_5$, where M is Mg^{+2}, Fe^{+2}, Mn^{+2}, or Co^{+2}.

Pyroborate compounds have also been investigated by Takeuchi [4], who determined the crystal structure of suanite, which is the monoclinic form of magnesium pyroborate. He also suggested parameters for the triclinic form. These parameters differed slightly from those determined by Berger for $Co_2B_2O_5$ [2]. It was deemed desirable to refine the structural parameters of the $Mg_2B_2O_5$ in order to define the $B_2O_5^{-4}$ configuration accurately. In the X-ray scattering process the form factor is proportional to the atomic number. Thus the Mg:B scattering ratio presented the most favorable case in the isomorphous series for elucidating the pyroborate configuration.

[1] Figures in brackets indicate the literature references at the end of this paper.

2. Experimental Techniques

Single crystals of $Fe_2B_2O_5$ and both phases of $Mn_2B_2O_5$ were obtained by crystallization from the melt and cell constants obtained on a Buerger precession camera. The single crystals of $Mg_2B_2O_5$ used were either taken directly from a devitrified glass or recrystallized from it. Data was obtained on a Nonius integrating Weissenberg camera using Cu K_α radiation. Zero layers and *b*-axis upper layers were taken. Integrated intensities were read directly on a densitometer comparator. Lorentz-polarization corrections were applied according to the method given by Lu [5].

3. Structure

3.1. Space Group and Cell Constants

$Mg_2B_2O_5$ crystallizes in the triclinic system, space group $P\bar{1}$. The cell dimensions were obtained from single-crystal precession and Weissenberg data.

The cell constants for the four members of the isomorphous series are given in table 1. For the $Mg_2B_2O_5$ the cell volume is 172.0 A^3 and the calculated density for two formula units per cell is 2.90 g/cm^3 (observed 2.92 g/cm^3).

TABLE 1. *Cell constants for triclinic phases*

	a	*b*	*c*	α	β	γ
$Mg_2B_2O_5$	6.18$_7$	9.21$_9$	3.11$_9$	90°24′	92°08′	104°19′
$Mn_2B_2O_5$	6.26$_6$	9.57$_5$	3.27$_1$	90°34′	91°53′	104°55′
$Fe_2B_2O_5$	6.18$_2$	9.40$_4$	3.25$_8$	90°37′	91°29′	104°10′
$Co_2B_2O_5$	5.94	8.95	3.16	91°0′	92°0′	103°54′
Monoclinic						
$Mn_2B_2O_5$ $P2_1/c$	3.25$_2$	9.53$_7$	9.90$_3$	-----	110°00′	------

3.2. Structure Determination

The only well resolved projection of the electron density for this structure was on the plane containing the *a* and *b* axes, i.e., on (001). Preliminary refine-

ment was carried out by use of successive Fourier projections. The signs for the structure factors were derived from the trial structure analogous to the $Co_2B_2O_5$, with Mg replacing the Co. The final Fourier projection is shown in figure 1. At this stage the reliability factor R, defined as

$$R=\Sigma||F_o|-|F_c||/\Sigma|F_o|$$

was 0.125 for the 99 observed $hk0$ nonzero reflections. The structure was in good agreement with the corresponding Patterson projection (fig. 2). It is essentially the same structure as proposed by Takeuchi, with the origin shifted by $(\frac{1}{2},\frac{1}{2},0)$.

The final stages of refinement consisted of a least-squares reduction of the data, using the electronic computer and the NYXRIA routine written by Sayre [6] and revised by Vand [7]. The zero and 4 upper levels of Weissenberg data around the b axis were used. The final R value for the $Mg_2B_2O_5$ structure is 0.123, using 331 nonzero independent reflections. An isotropic temperature factor for each atom was used. The atomic coordinates and temperature factors are listed in table 2. Measured and calculated structure factors are given in table 3.

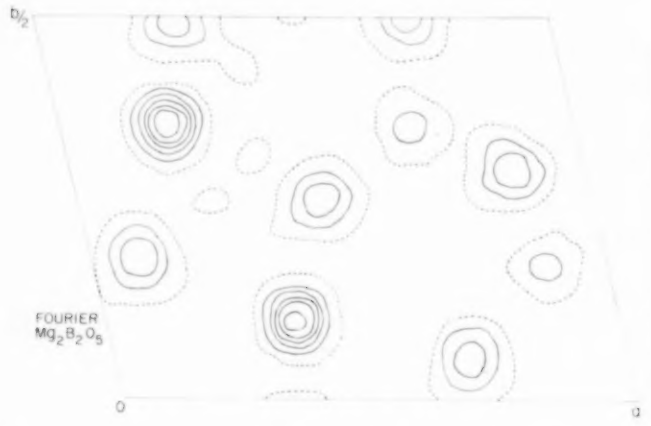

FIGURE 1. *Fourier projection of* $Mg_2B_2O_5$ *on the (001) plane.*

In order of increasing number of contour lines the atoms are B, O, and Mg. Half the unit cell is shown for the centrosymmetric space group.

FIGURE 2. *Patterson projection of* $Mg_2B_2O_5$ *on the (001) plane.*

TABLE 2. *Atomic coordinates of triclinic* $Mg_2B_2O_5$

	x/a	y/b	z/c	B
Mg_1	0.2105	0.3562	0.7264	0.70 Å^2
Mg_2	.3724	.1026	.2345	.68
O_1	.6972	.0511	.2631	.89
O_2	.0931	.1784	.2263	.89
O_3	.4782	.2595	.7376	.79
O_4	.8633	.2995	.5604	.97
O_5	.7224	.5077	.7709	.78
B_1	.6836	.3538	.6997	.33
B_2	.8814	.1708	.3392	.37

TABLE 3. *Calculated and observed structure factors for triclinic* $Mg_2B_2O_5$

$k=0$

h \ l	0	+1	+2	+3
−7		−120 [a] 191		
−6			+23 28	
−5		−86 96	+39 39	+29 37
−4		+228 268	−26 14	−77 87
−3		+295 339	−68 58	−120 124
−2		−91 87	+140 140	+76 83
−1		−22 21	+205 249	+16 14
0		−156 214	−532 670	+33 39
+1	−63 75	−134 170	+74 87	
+2	−259 285	+160 190	+139 144	−140 161
+3	−33 40	+110 110	−70 68	+63 69
+4	−85 86	−134 131		
+5	−74 71	+135 146		
+6	+20 28	−40 52		
+7	−57 71			

[a] Numbers with signs are calculated structure factors and numbers without signs are observed values.

TABLE 3. *Calculated and observed structure factors for triclinic* $Mg_2B_2O_5$—Continued

$k=1$

h \ l	−2	−1	0	+1	+2	+3
−7			−35 33	−101 102		
−6		−291 279	+163 172	+221 222	−120 120	
−5	+56 44	−46 40	+68 67			
−4	+208 161	−60 54	−312 286	+52 48	+293 296	−102 94
−3	−232 189	+108 85	+213 218		−95 90	−54 48
−2		+101 95	+79 84	+80 95	−126 125	
−1		+242 267	+3 34	−15 30	−118 99	
0			+27 26	+88 91	−159 157	
+1		−23 36	−173 173	−147 173	+204 183	+97 101
+2	−62 61		+227 233	−164 169		
+3		−243 257	+128 129	−396 424	−57 56	+166 165
+4	+83 72	−377 428	−93 99	+294 319	+37 40	−127 140
+5		−16 41	−107 127	+145 157	+50 61	
+6	+46 41	+172 208	−139 151	−59 64	+52 45	
+7				+28 28		

$k=2$

h \ l	−2	−1	0	+1	+2	+3
−6		+27 26	−21 23	+52 53	−16 20	
−5	+113 103		−116 112		+43 38	+52 41
−4	−85 66	−68 48	+187 172	−21 23	−57 55	+47 37
−3	−231 193	+8 22	+634 600	−132 115	−367 323	
−2		−109 101	−399 332	+30 27	+232 227	−101 98
−1		−21 22	−134 107	+113 106	+128 112	−143 132
0		+134 144	−134 107	−468 489	+35 30	+168 175
+1	−46 37	+74 78	−120 119		−38 40	+85 82
+2		−236 214	−99 105	+228 194	−59 54	−19 26
+3	+74 61	−58 56		−32 33	+21 24	+63 58
+4	+135 142	−206 218	−75 72	+142 125	+110 112	−107 89
+5	−54 59	+53 64	+140 145	−110 127	−63 59	
+6	−3 22		−23 26	−33 38		

$k=3$

h \ l	−2	−1	0	+1	+2	+3
−7		−32 34	−119 120	+34 39		
−6		+125 152	+256 299	−127 144	−135 169	
−5	−47 49	+63 71		−20 24	−23 25	+25 20
−4	−29 32	−44 41		+123 128	−124 108	−11 22
−3	+114 115		−76 81		−67 65	+77 75
−2		+21 23	−138 113	−93 100	+142 129	+68 81
−1			+91 55	−123 124	−37 31	
0		+134 144	+45 39	−377 426	+27 31	+138 144
+1			−145 123	+496 513	+158 168	−274 298
+2		−174 174	−129 134	+41 37	+63 62	−92 72
+3		+204 200	−159 156	−138 131	+69 66	+124 132
+4	−183 194	−51 51	+158 142	+40 46	−91 107	
+5	−49 60	−106 115	+168 191	+89 100	−159 179	
+6		−55 58	−43 54			

$k=4$

h \ l	−3	−2	−1	0	+1	+2
−7			+40 47	+96 105	−28 41	
−6		−25 28		−153 135	−53 63	−125 135
−5		+154 158	−85 94	−195 151	+12 24	+205 192
−4		−80 68	+82 69		−38 41	+83 69
−3	−129 140		+432 339	−73 70	−390 282	
−2	+230 228	−70 73	−252 218	+5 12	+230 191	−118 102
−1	+45 63	+56 34	−195 176	−153 109	+283 232	
0	−63 66	+196 172	−100 89	−106 85		
+1		+58 60	−139 138	+24 47	+69 58	
+2	−94 109	−127 117	+134 131	+194 182	−216 176	
+3	+51 52		−39 29	−35 34		
+4		−209 215	−54 52	+233 231	+100 103	
+5		+80 108	+136 134	−140 157	−80 76	
+6			+47 65	−103 131		

TABLE 3. *Calculated and observed structure factors for triclinic* $Mg_2B_2O_5$—Continued

$l=0$

k \ h	−7	−6	−5	−4	−3	−2	−1	0	+1	+2	+3	+4	+5
5		−157 128	−53 40	+168 76				−216 198	+308 279	+114 113	−162 180		
6		−35 40		−103 87	−108 95	+119 106	+223 209	+101 96	+212 204	−362 362	−36 50	+122 149	−74 80
7	+41 52		+48 41	−81 67	−155 134	+362 310	−90 77	−176 182	+145 147	+61 61		−80 105	
8		−62 65	+145 146	+166 161			−317 300	+65 76	+48 41	−49 50		+39 63	
9			+213 216	−178 186		+111 107		−49 50	−112 120	−91 92	+93 117		
10			−35 43	−121 121	+85 85					+53 73			
11				+25 33		−83 85							

3.3. Accuracy of Parameters

Assuming a 15-percent error in the corrected observed intensities and an isotropic coordinate error the average standard deviations of the bond lengths, estimated by the method of Cruickshank [8] are

$$\sigma_{B\text{-}O}=0.018 \text{ A}$$
$$\sigma_{O\text{-}O}=0.011 \text{ A}$$
$$\sigma_{Mg\text{-}O}=0.009 \text{ A}.$$

4. Description of the Structure

4.1. General

The structure of $Mg_2B_2O_5$ consists of discrete pyroborate groups and Mg^{+2} ions. Each magnesium is surrounded octahedrally by six oxygen atoms. Sets of four octahedra are linked by edge sharing and propagated in the direction approximately parallel to (110). These are extended in infinite slats parallel to the c direction by edge sharing with the octahedra in the cells immediately above and below (fig. 3). The pyroborate groupings extend this pattern through $O_{IV}-B_I-O_V$ into an extended sheet. The slats of octahedra are also linked normal to the propagation direction by the pyroborate groups. This cross linkage is through $O_I-B_{II}-O_{II}$ and $O_{III}-B_I-O_{IV}$.

4.2. Pyroborate Group

Each boron atom is in triangular coordination with three oxygen atoms. The pyroborate group consists of two such triangles with one shared oxygen (fig. 4). In this coordination type boron should form three coplanar bonds utilizing sp^2 hybridization, with interbond angles of 120°. In the $Mg_2B_2O_5$ structure, the two triangles are not identical. Each has a different environment and nonsymmetric bond lengths. The $O_{II}-O_{IV}$ distance is shorter than all other edges of the triangles. This is, however, the only edge of a triangle within the pyroborate group which is shared with an edge of a magnesium octahedron. Within each triangle there are two B–O distances averaging 1.39 A and one somewhat shorter at about 1.36 A. The mean value of all six B–O bonds is 1.38$_4$. Within the $B_2O_5^{-4}$ group. the $B_I-O_{IV}-B_{II}$ angle is 134.5° and the angle between the planes of the triangles is 16°. B_I and B_{II} are within 0.03 and 0.02 A, respectively, of the planes determined by the three coordinated oxygens.

The two outer oxygens in the triangle surrounding B_{II} are coordinated as expected to six magnesium atoms while the two peripheral oxygen atoms in the triangle surrounding B_I are coordinated to only five magnesium atoms. The center O_{IV} is bound to both borons as well as one Mg. O_V is only bonded to two magnesium atoms, as well as the central boron. All other oxygens are tied to one boron and three magnesiums.

According to Pauling's electrostatic rules the strength of a bond from a cation to an anion is z/CN, where z is the charge and CN the coordination number. (This rule is only strictly applicable for equal bond lengths and symmetric geometric arrangements.) Each boron atom is tied to three oxygens; the bond strength is 3/3. Each magnesium is bonded to six oxygens; the bond strength is $2/6=1/3$. The total charge on the anion must be neutralized in the bonds, or a charge disproportionation occurs. O_I, O_{II}, and O_{III} are each bound to three Mg and one B atoms. Thus their charge is neutral. The O_V, bound to two Mg and one B, has a $-1/3$ charge. The O_{IV} is tied to both borons as well as one Mg. Thus it has a $+1/3$ excess charge, indicating a deviation from Pauling's rule. These bond strengths are based on an equalized distribution. Since the bond lengths vary they represent only an idealized situation. Thus the charge on O_V is probably equalized by the closer approach of the two Mg atoms. These same Mg are then bonded rather more loosely to the O_{IV} and O_{II} atoms.

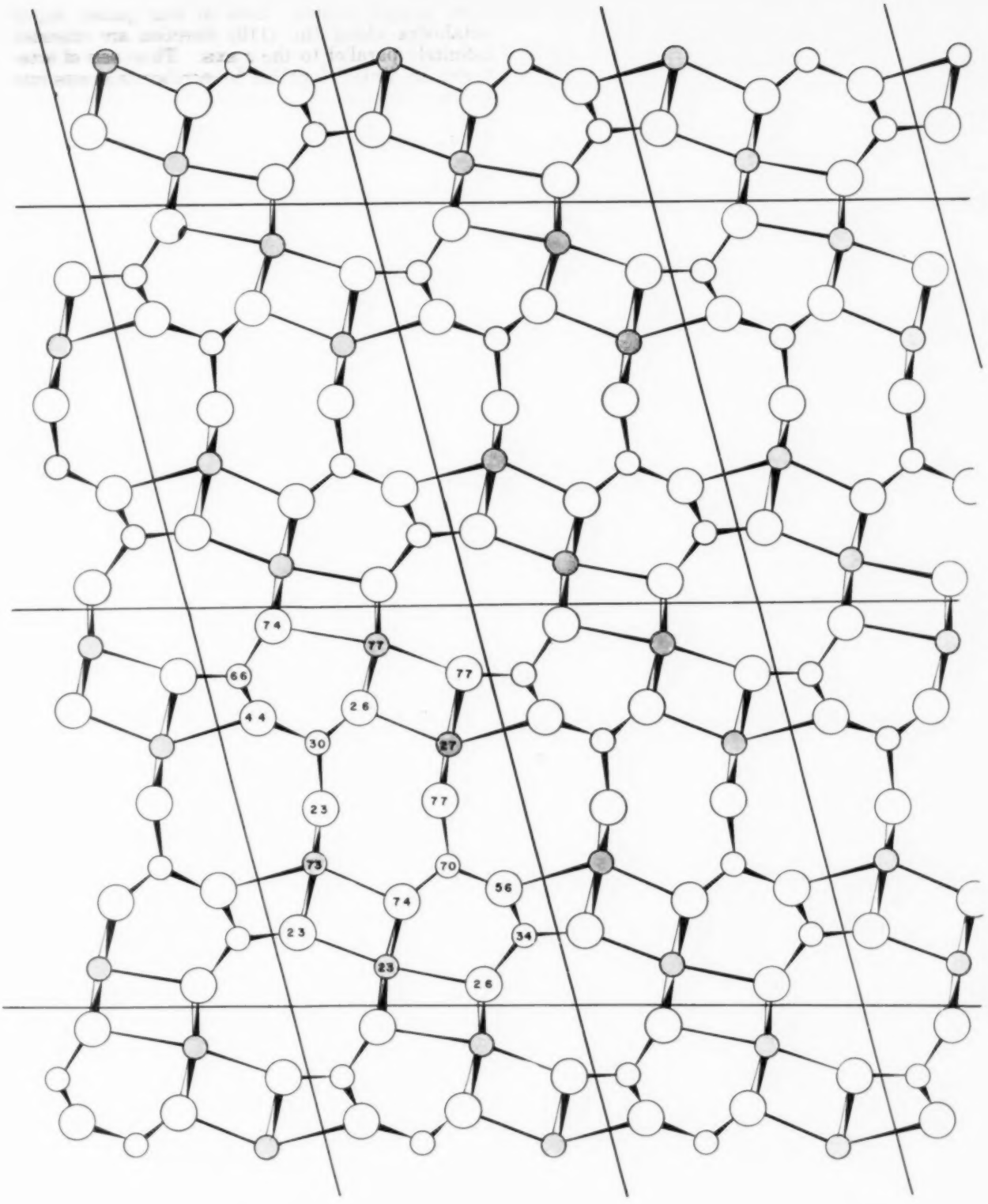

FIGURE 3. *Projection of the structure of* $Mg_2B_2O_5$ *on the (001) plane (x positive to the right, y positive toward the top).*

Shaded circles are Mg, small circles B, large circles O. The numbers indicate the *z* parameter.

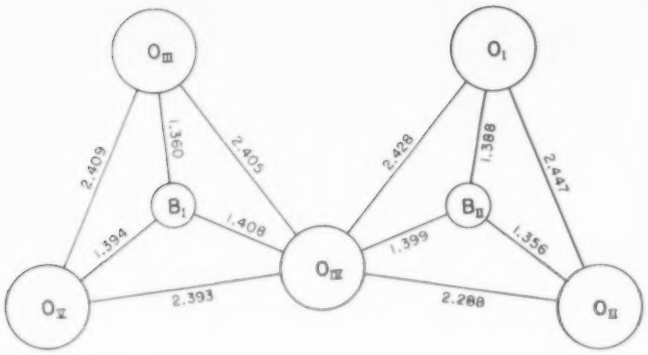

FIGURE 4. *Projection of the pyroborate group showing all interatomic distances in angstrom units.*

The best refined borate structure to date appears to be that of orthoboric acid [9]. This structure consists of discrete BO_3^{-3} triangles and the average of all B–O bond distances obtained was 1.361 A. This may be compared with the 1.38_4 average oxygen-boron distance obtained for $Mg_2B_2O_5$ above. The average O–O interatomic distance within a BO_3^{-3} triangle for boric acid is 2.356 A, compared to 2.395 A in the present structure.

5. Summary

The triclinic modification of magnesium pyroborate $Mg_2B_2O_5$ has been shown to be a member of an isostructural series, the other members of which are $Mn_2B_2O_5$, $Fe_2B_2O_5$, and $Co_2B_2O_5$. The atomic parameters of the $Mg_2B_2O_5$ have been refined by Fourier and least-squares techniques.

The structure consists of $B_2O_5^{-4}$ groups and Mg^{+2} ions. Each magnesium has a sixfold coordination with oxygen atoms. Sets of four joined Mg–O octahedra along the (110) direction are extended infinitely parallel to the *c* axis. These sets of octahedra are linked together by pyroborate groups into sheets approximately along (110) with cross linking normal to this direction.

The pyroborate group consists of two joined BO_3^{-3} triangles sharing one corner oxygen. The B–O–B angle is 134.5° and the boron atoms are in the plane defined by the three surrounding oxygens.

Within the limits of error, all B–O distances are equivalent. One side of a triangle is significantly shortened because of edge sharing with a magnesium octahedron.

The authors thank C. T. Ireland for performing some of the earlier computations and Peter O'Hara for aid during the computing procedures. E. M. Levin pointed out the relationship of the phase diagram and correct molecular formula.

6. References

[1] ASTM X-ray powder data file cards numbers: 3–0841, 3–0815, 3–0186.
[2] S. V. Berger, Acta Chem. Scand. **4,** 1054 (1950).
[3] H. M. Davis and M. A. Knight, J. Am. Ceram. Soc. **28,** 100 (1945).
[4] Y. Takeuchi, Acta Cryst. **5,** 574 (1952).
[5] C. S. Lu, Rev. Sci. Instr. **14,** 331 (1943).
[6] D. Sayre, IBM (personal communication).
[7] V. Vand, The Penna. State Univ. (personal communication).
[8] D. W. J. Cruickshank, Acta Cryst. **2,** 65 (1949).
[9] W. H. Zachariasen, Acta Cryst. **7,** 305 (1954).

WASHINGTON, October 30, 1958.

Journal of Research of the National Bureau of Standards Vol. 62, No. 3, March 1959 Research Paper 2937

Heat Transfer in Laminar Flow Through a Tube[1]

Milton Abramowitz,[2] William F. Cahill,[3] and Clarence Wade, Jr.[3]

The problem of heat transfer due to laminar flow of a viscous fluid in a channel is studied under the assumption that there is a parabolic distribution of velocity. The effect of axial temperature changes are considered and the solution is based on the simpler situation where axial effects are discussed. The solution, obtained by the method of least squares, is represented in terms of a set of nonorthogonal characteristic functions. These functions and the corresponding characteristic values are determined by numerical integration employing the Runge-Kutta procedure. Finally, asymptotic developments are obtained which are useful in the limiting cases.

1. Statement of Problem

The present paper is concerned with the steady state problem of heat transfer in a tube. The fluid moves with a prescribed velocity profile, which is parabolic in the present case. Thus the end effect is not considered in the velocity profile. The heat transfer is small and is supposed not to influence the fluid motion. The wall of the tube is assumed to be kept at a fixed temperature, θ_1, while the temperature of the fluid entering the tube is fixed to be θ_0. The velocity distribution in the tube whose radius is unity is defined by

$$v_z=2v_m(1-r^2),\ 0\leq r\leq 1, \tag{1.1}$$

where r is the radial distance from the center and v_z is taken along the x-axis which is the axis of symmetry of the tube and v_m is the average value of v_z. The equation of heat transfer under these conditions is

$$v_z\frac{\partial\theta}{\partial x}=K\left\{\frac{\partial^2\theta}{\partial r^2}+\frac{1}{r}\frac{\partial\theta}{\partial r}+\frac{\partial^2\theta}{\partial x^2}\right\} \tag{1.2}$$

with the boundary conditions

$$\begin{aligned}\theta&=\theta_0 \text{ for } x=0\\ \theta&\text{ finite for } x=\infty\\ \theta&=\theta_1 \text{ for } r=1.\end{aligned} \tag{1.3}$$

This problem has been considered [1][4] under the assumption that temperature changes in the x-direction will be negligible so that the term $\partial^2\theta/\partial x^2$ may be omitted. However, recent studies [2,3], which have included the effects of this term have exhibited solutions based on approximating the temperature distribution by a series of Bessel functions. In the present paper we propose to obtain a solution by the method of least squares. The boundary value problem will be solved by numerical integration of the differential equation employing the Runge-Kutta method. This procedure avoids the use of special functions but employs the basic concepts necessary to solve the boundary value problem. The results obtained indicate that the present technique may be employed in other problems of a similar nature.

Let us first put $\lambda=2v_m/K$ and $\lambda\xi=x$ so that (1.2) becomes

$$(1-r^2)\frac{\partial\theta}{\partial\xi}=\frac{\partial^2\theta}{\partial r^2}+\frac{1}{r}\frac{\partial\theta}{\partial r}+\frac{1}{\lambda^2}\frac{\partial^2\theta}{\partial\xi^2} \tag{1.4}$$

while the boundary conditions (1.3) remain unchanged except that x is replaced by ξ. We see from (1.4) that when λ increases the contribution from the term $\partial^2\theta/\partial\xi^2$ will decrease. By analogy with the solution for $\lambda=\infty$ it is assumed that

$$\frac{\theta-\theta_1}{\theta_0-\theta_1}=\sum_{n=1}^{\infty}A_n\exp(z_n\xi)y(r,z_n), \tag{1.5}$$

where the constants z_n are the eigenvalues and the functions $y(r,z_n)$ are the eigenfunctions of the boundary value problem

$$y''+\frac{1}{r}y'+\left\{\frac{z_n^2}{\lambda^2}-z_n(1-r^2)\right\}y=0, \tag{1.6}$$

$$y(r,\lambda,z)=0 \text{ for } r=1. \tag{1.7}$$

[1] The preparation of this paper was sponsored in part by the Office of Naval Research, United States Navy.

[2] Deceased.

[3] Present address, Theoretical Division, National Aeronautics and Space Administration.

[4] Figures in brackets indicate the literature references at the end of this paper.

TABLE 1. *The eigenvalues*—z_n

n	$\lambda^a=0$	$\lambda=1$	$\lambda=10$	$\lambda=100$	$\lambda=1000$	$\lambda=\infty$
1	2.405	2.644369	6.744051	7.306909	7.313523	7.313587
2	5.520	5.187345	30.76791	44.32333	44.60653	44.66947
3	8.654	8.323452	59.50344	111.9926	113.9009	113.9210
4	11.792	11.46137	89.47665	208.3608	215.1669	215.2447
5	14.931	14.60050	119.9727	330.8685	348.3678	348.564
6	18.071	17.74037	150.7501	476.6471	513.4475	513.890
7	21.212	20.88073	181.6979	642.7513	710.3849	711.217
8	24.352	24.02119	212.7574	826.6381	939.7287	940.551
9	27.49	27.16301	243.9199	1024.875	1196.191	1201.87
10	30.63	30.30613	275.1170	1224.774	1464.309	1495.20
11	33.78	33.44743				
12	36.92	35.50123				
13	40.06	40.06675				

[a] For $\lambda=0$, z_n are the zeros of the Bessel function $J_0(z)$; the values for $\lambda=\infty$ were taken from reference [4].

In order to have axial symmetry it is required that $y(r,\lambda,z)$ be an even function of r. Further, to determine the temperature distribution θ in (1.5), we determine solutions of (1.6) which constitute a nonorthogonal set of characteristic functions $y(r, \lambda,z_n)$. It is noted that since z occurs quadratically in (1.6) there are two sets of characteristic values. It turns out that one set is all positive while the other is all negative. However, in evaluating the temperature distribution, we wish to have a solution which is finite for ξ infinite so we discard the positive set of characteristic values. In order to satisfy the condition $\theta=\theta_0$ at $\xi=0$ we formally assume the solution in the form

$$f(r)\sim\sum_{n=1}^{\infty}A_n y(r,z_n), \tag{1.8}$$

where $f(r)=1$ in the present problem. When $\lambda=\infty$, (1.6) reduces to the Graetz-Nusselt equation and the functions $\sqrt{r(1-r^2)}$, $y(r,z_n)$ constitute an orthogonal set and the coefficients are determined accordingly. In the present case where λ is finite the orthogonality property no longer holds. However, we may still determine the coefficients in the sense of least squares. Consequently, we require

$$\int_0^1 r(1-r^2)\left\{f(r)-\sum_{n=1}^{\infty}A_n y(r,z_n)\right\}^2 dr=\text{minimum}. \tag{1.9}$$

The weight function $r(1-r^2)$ has been introduced so that the results shall be consistent with the Graetz-Nusselt ($\lambda=\infty$) case. It should be noted that the solution of (1.6) may be expressed in terms of the confluent hypergeometric function. However, to obtain the required results it would still be necessary to consider the problem of evaluating these functions. Instead, we propose to solve the differential eq (1.6) directly using numerical integration. Differentiating (1.9) with respect to A_n we get the infinite system of equations

$$\alpha A=\beta, \tag{1.10}$$

where

$$\alpha=[\alpha_{mn}]=\left[\int_0^1 r(1-r^2)\ y(r,z_m)\ y(r,z_n)dr\right],$$

$$\beta=[\beta_m]=\left[\int_0^1 r(1-r^2)\ y(r,z_m)\ f(r)dr\right],$$

$$A=[A_n],m,n=1,2,\ \ldots\ . \tag{1.11}$$

2. Determination of z_n and $y(r,z_n)$

The solution of the infinite system is dependent on the determination of the characteristic functions $y(r,z_n)$ and the characteristic values z_n. The power series solution of (1.6) is

$$y(r,z_n)=\sum_{k=0}^{\infty}b_{2k}r^{2k}, \tag{2.1}$$

where

$$b_0=1,b_2=-\frac{1}{4}\left(\frac{z^2}{\lambda^2}-z\right),4k^2b_{2k}+(z^2/\lambda^2-z)b_{2k-2}+zb_{2k-4}=0. \tag{2.2}$$

This representation was used to expedite the numerical integration of (1.6). The Runge-Kutta method [5] was employed starting at $r=0.5$ with the value of $y(0.5,z_n)$ obtained from (2.1) with trial values of z_n. The results are given in table 1 (see figure 1 for the characteristic functions corresponding to $\lambda=10$).

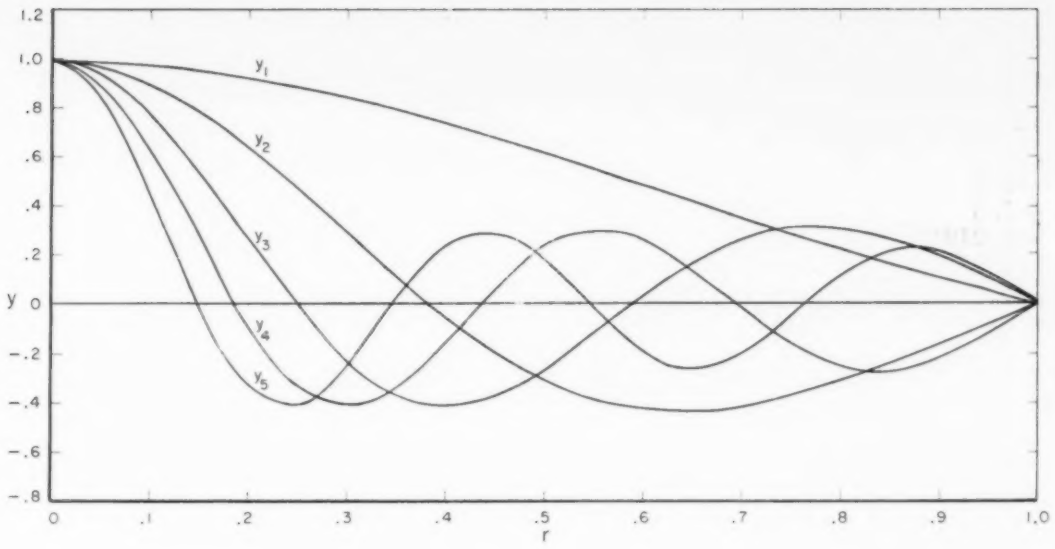

FIGURE 1.

3. Calculation of the Coefficients A_j

The integrals in (1.11) necessary for the determination of the solution A of (1.10) were evaluated with Simpson's rule using the characteristic functions $y(r, z_n)$ calculated previously. We give the results obtained for 3 cases. Since the matrices are symmetric we omit the elements above the main diagonal.

$\lambda=1, \quad m=n=5$

$$10^5\alpha=(10^5\alpha_{mn})=\begin{bmatrix} 1018886 & & & & \\ 1338862 & 3951938 & & & \\ -242794 & 849201 & 2472921 & & \\ 77045 & -176352 & 606464 & 1804961 & \\ -32588 & 63431 & -133686 & 469689 & 1422473 \end{bmatrix}$$

$\lambda=10, \quad m=n=5$

$$10^7\alpha=(10^7\alpha_{mn})=\begin{bmatrix} 947286 & & & & \\ 42284 & 382270 & & & \\ -18966 & 48645 & 239335 & & \\ 8546 & -16907 & 43600 & 175401 & \\ -4079 & 7130 & -13791 & 37374 & 138567 \end{bmatrix}$$

$\lambda=1000, \quad m=n=8$

$$10^7\alpha=(10^7\alpha_{mn})=\begin{bmatrix} 939335 & & & & & & & \\ 5 & 375196 & & & & & & \\ -12 & 15 & 234420 & & & & & \\ 6 & -19 & 26 & 170471 & & & & \\ -11 & 11 & -28 & 39 & 133932 & & & \\ 6 & -17 & 19 & -43 & 66 & 110280 & & \\ 8 & 3 & -32 & 33 & -35 & 38 & 93796 & \\ 52 & -14 & -69 & 120 & 157 & 158 & -186 & 81323 \end{bmatrix}$$

Thus for $\lambda=1$, if we start with the approximations $z_2^{(1)}=-5$ and $z_2^{(2)}=-6$ to z_2 the following successive approximations are obtained:

j	$z_2^{(j)}$	$y(1,z_2^{(j)})$
1	−6.0	0.2362897
2	−5.0	$-.6633393\times10^{-1}$
3	−5.219196	$.1110549\times10^{-1}$
4	−5.187761	$.1455328\times10^{-3}$
5	−5.187344	$-.4580215\times10^{-6}$
6	−5.187345	$-.2379238\times10^{-7}$

The improved value of z_n was obtained by linear interpolation as follows:

$$\frac{z_2^{(j+1)}-z_2^{(j)}}{z_2^{(j-1)}-z_2^{(j)}}=\frac{y(1,z_2)-y(1,z_2^{(j)})}{y(1,z_2^{(j-1)})-y(1,z_2^{(j)})};y(1,z_2)=0.$$

The efficiency of the method was dependent on the choice of the initial values of z. Once some of the eigenvalues were known, relatively good starting values were easily found by extrapolation. In performing the integration (1.6) was written in the form

$$y'=\frac{1}{r}u$$

$$u'=-r\{(z^2/\lambda^2-z)+zr^2\}y$$

and the interval $\Delta r=0.002$ was ultimately employed.

It is noted that as λ increases, the matrix α tends to a diagonal matrix, i.e., the set of characteristic functions $y(r, z_n)$ tends to an orthogonal set with respect to the weight factor $r(1-r^2)$. Finally, examination of the integrals which are the elements of α and β indicates that since $f(r)=1$, elements of β follow as a simple byproduct of the computation of the elements of α.

Solving the system $\alpha A=\beta$ we get the values of A_n in table 2.

With the known values of A_n we are able to test the efficiency of the least square approximation. The results are summarized in table 3.

We conclude from the above that the method described yields satisfactory results for practical purposes. In conclusion we shall give asymptotic representations useful in the regions of small and large values of λ. These serve to confirm the numerical results obtained previously.

TABLE 3. $\sum_{n=1}^{\infty}A_n y(r,z_n)\sim f(r)=1$

r	$\lambda=1$		$\lambda=10$		$\lambda=100$		$\lambda=1{,}000$	
	$n=5$	$n=8$	$n=5$	$n=8$	$n=5$	$n=8$	$n=5$	$n=8$
0	0.981	0.918	1.151	0.905	1.188	0.845	1.188	0.864
0.1	.937	1.011	1.047	1.009	1.037	1.042	1.033	1.100
.2	.909	1.004	0.935	0.997	0.921	0.972	0.922	0.961
.3	1.004	0.985	1.001	.992	1.042	1.033	1.186	1.178
.4	1.100	1.023	1.057	1.010	1.040	0.965	1.036	0.963
.5	1.053	0.971	0.969	0.972	0.920	1.023	0.917	1.036
.6	0.965	1.032	.942	1.039	.997	0.997	1.004	0.974
.7	.990	0.969	1.076	0.952	1.139	.964	1.142	.987
.8	.984	1.024	1.081	1.052	0.992	1.121	0.983	1.126
.9	.651	1.004	0.682	0.964	.539	0.758	.528	0.718
1.0	0	0	0	0	0	0	0	0

4. Solution of (1.6) for Small Values of λ

To obtain a solution of (1.6) in terms of Bessel functions valid for small values of λ we put $\alpha\lambda=z$ and obtain

$$y''+r^{-1}y'+[\alpha^2-\alpha\lambda(1-r^2)]y=0. \qquad (4.1)$$

Now if $\lambda\to0$, (4.1) becomes $y''+r^{-1}y'+\alpha^2y=0$. The solution of the limiting problem is $J_0(\alpha_s r)$ where J_0 is the Bessel function of the first kind of order zero and $\alpha_s=j_s$ are the zeros of J_0.

TABLE 2. *Values of* A_n

n	$\lambda=1$		$\lambda=10$		$\lambda=100$		$\lambda=1{,}000$	
	$n=5$	$n=8$	$n=5$	$n=8$	$n=5$	$n=8$	$n=5$	$n=8$
1	1.5779	1.6003	1.5370	1.5423	1.478413	1.479273	1.476457	1.476472
2	−0.9629	1.0527	−0.9563	−0.9778	−0.8126151	−0.813778	−0.806192	−0.806222
3	.5217	0.8172	.7559	.8062	.599728	.606701	.588885	.588874
4	−.4547	−.6658	−.5894	−.6865	−.488371	−.501968	−.475988	−.475937
5	.2995	.5489	.4038	.5805	.411076	.419506	.405103	.405024
6		−.4462		−.4797		−.390254		−.355635
7		.3450		.3765		.348450		.318681
8		−.2289		−.2565		−.303294		−.287201

Thus, if we assume

$$y(r)=y_0+\lambda y_1+\lambda^2 y_2+ \ . \ . \ .$$

$$\alpha_s(\lambda)=\alpha_{0s}+\lambda\alpha_{1s}+\lambda^2\alpha_{2s}+ \ . \ . \ . \qquad (4.2)$$

and substitute in (4.1) we find

$$y_1(r)=\left(\frac{1}{6}-\frac{1}{3j_s^2}\right) r\, J_1(j_s r)-\frac{1}{2}\frac{r^2}{j_s^2}\, J_2(j_s)+\frac{r^3}{6}\, J_3(j_s)$$

$$\alpha_{1s}=\frac{1}{3}+\frac{1}{3j_s^2},\ \alpha_{2s}=\frac{1}{15j_s}-\frac{7}{90j_s^3}+\frac{59}{90j_s^5}. \qquad (4.3)$$

Omitting further approximations we show the comparison considering the quantities α_{1s} and α_{2s}.

λ	$-z_1(\lambda)$	*Approx.*	$-z_2(\lambda)$	*Approx.*
1	2.04437	2.04417	5.187345	5.18755
2	3.48773	3.44802	9.75388	9.7570
5	5.68968	6.0350	20.4943	20.462
10	6.744051	15.2	30.7679	32.52

5. Solution of (1.6) for Large Values of λ

Let us assume that

$$y(r)=y_0+\lambda^{-2}y_1+\lambda^{-4}y_2+ \ . \ . \ .$$

$$z_s(\lambda)=-z_{0s}+z_{1s}\lambda^{-2}+z_{2s}\lambda^{-4}+ \ . \ . \ .$$

We then find that $y_0(r)$ is the solution of the Graetz-Nusselt equation and z_{0s} are the corresponding eigenvalues which have been listed in table 1. Substituting in (1.6) we obtain a series of characteristic values from which we find

s	z_{1s}	z_{2s}
1	−66.9260	1218.6
2	−2897.8	374×10^3

A comparison of the results taking into account z_{1s} and z_{2s} follows:

λ	$-z_1(\lambda)$		$-z_2(\lambda)$	
	True value	*Approx.*	*True value*	*Approx.*
10	6.744	6.766	30.8	53.0
100	7.307	7.307	44.3	44.323
1000	7.3135	7.313	44.6065	44.606
∞	7.313587		44.60947	

The authors acknowledge suggestions and assistance of Miss Irene A. Stegun in the asymptotic developments obtained.

6. References

[1] M. Jakob, Heat transfer, vol. 1 (John Wiley & Sons, Inc., New York, N.Y., 1949), p. 451.

[2] K. Millsaps and K. Pohlhausen, Heat transfer to Hagen-Poiseuille flows, Proceedings of the Conference on Differential Equations (University of Maryland, College Park, Md., 1955).

[3] S. N. Singh, Heat transfer by laminar flow in cylindrical tube (private communication).

[4] M. Abramowitz, On the solution of the differential equation occurring in the problem of heat convection in laminar flow through a tube, J. Math. Phys. **32**, 184 (1953).

[5] William E. Milne, Numerical solution of differential equations, Ch. 5 (John Wiley & Sons, Inc., New York, N.Y., 1953).

[6] H. A. Lauwerier, The use of confluent hypergeometric functions in mathematical physics and the solution of the eigenvalue problem, Appl. Sci. Research, [A] **2**, 184 (1951).

Washington, June 2, 1958.

Journal of Research of the National Bureau of Standards Vol. 62, No. 3, March 1959 Research Paper 2938

Fluorination of Haloaromatic Compounds[1,2]

Roland E. Florin, Walter J. Pummer, and Leo A. Wall

The reactions of BrF_3, ClF_3, and IF_5 with C_6Cl_6, C_6Br_6, C_6Cl_5–CF_3, and other haloaromatic compounds are described. These reactions are not readily controlled, and explosions frequently occurred, particularly when BrF_3 and ClF_3 were used. Dehalogenation of the reaction products led to certain aromatic fluorocarbons, for example, C_6ClF_5 and C_6ClF_4–CF_3. Completely fluorinated aromatic compounds were not easily obtained, and therefore the process is not recommended for the production of these species.

1. Introduction

Until the recent disclosure of new methods for preparing hexafluorobenzene [1–3] [3] the only published syntheses [4,5] of aromatic fluorocarbons were the conversions of hexachlorobenzene to hexafluorobenzene and of pentachloro-α,α,α-trifluorotoluene to octafluorotoluene by an indirect procedure involving addition of bromine trifluoride, exchange fluorination with antimony pentafluoride, and dehalogenation with zinc.

Attempts were made to modify the method so as to prepare reactive mono- and bi-functional derivatives, as well as the parent fluorocarbons. For example, it was hoped that the final product in the following scheme would be obtained:

$$C_6Br_6 \xrightarrow{BrF_3} C_6F_4Br_2 \xrightarrow{Zn} C_6F_4Br_2.$$

Previously, a synthesis of a compound of this type and its conversion to a polyphenyl of low molecular weight was reported [6] from this laboratory. However, the synthesis was extremely laborious. The present work was undertaken to find a shorter path to the desired compound, which it is anticipated would lead to the synthesis of thermally stable polymers. The compound prepared earlier was tetrafluoro-1,4-diiodobenzene [6], and in the present work it was expected and hoped that the *meta* and *ortho* isomers would also be obtained.

2. Results and Discussion

In trying to repeat this previously described preparation, difficulties were experienced in the later, high-temperature stages of the bromine trifluoride reaction. The conditions of temperature and concentration prescribed in the literature led to explosions very frequently, and less severe reaction conditions were insufficient for producing the desired degree of fluorination. It was concluded that the operations described in the original paper are very close to the margin of safety. Milder fluorinations were conducted with apparent safety, leading ultimately to very poor yields of the fluorocarbons but to satisfactory yields of their monochloro derivatives. The stages of these syntheses are identified in the following summary, in which most formulas represent merely typical or rough average composition:

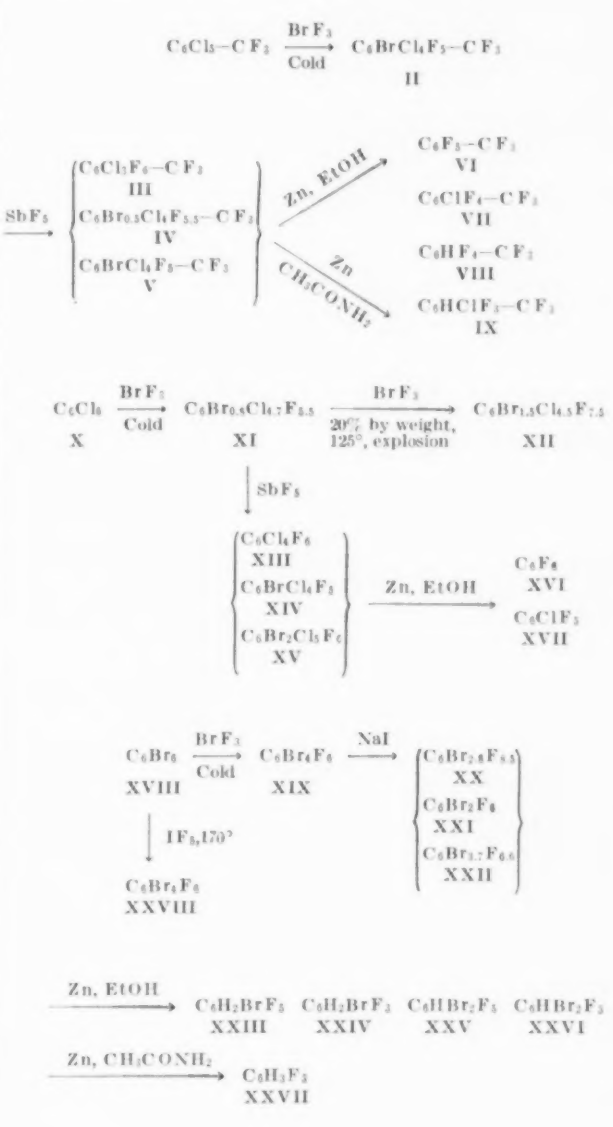

[1] This paper is based on work sponsored by the Ordnance Corps, Department of the Army, Washington, D.C.

[2] Presented as part of the Symposium on Fluorine Chemistry, Division of Industrial and Engineering Chemistry, at the 130th Meeting of the American Chemical Society, Atlantic City, N.J., September 1956.

[3] Figures in brackets indicate the literature references at the end of this paper.

The fluorination of hexabromobenzene proceeded smoothly, but subsequent reactions produced none of the desired perfluoroaromatic derivatives, although several new compounds were isolated. The scheme of synthesis requires that bromine trifluoride react only by addition, converting the original —CBr groups to saturated CFBr groups. From the behavior of the fluorination products, it appears that the bulk and lability of bromine hinder addition and favor replacement, leading to unreactive CF_2 groups. The following scheme accounts for some of the products:

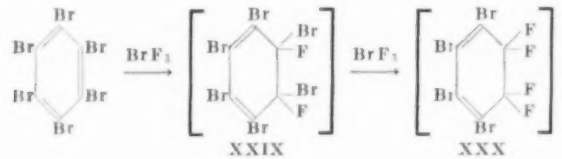

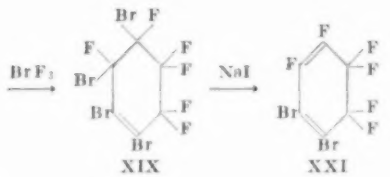

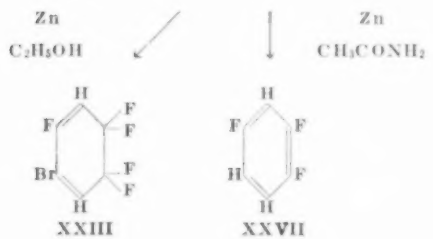

The hypothetical primary product XXIX contains "allylic" bromine atoms easily replaced.

A number of other polyhalogen derivatives of benzene were treated with halogen fluorides as well. The products from tetrahalobenzenes resembled those from the related hexahalobenzenes, but the fluorination was less easily managed. It was noticed that, during the zinc dehalogenation stage, some hydrogen is introduced into the ring when ethanol is the solvent; this occurs to a much greater extent with acetamide as solvent. The dehalogenation in acetamide of one lot of intermediate, approximately $C_6Br_2F_6$ (XXI), resulted in a large yield of a trifluorobenzene, boiling point 83° C, identified by its ultraviolet and mass spectra. The precursor of the trifluorobenzene is not clear. Its formation probably involves the replacement of "aromatic" or "unsaturated" bromine by hydrogen. This replacement is known to be effected by zinc plus mild acid [7] and occasionally by the action of bases on "aromatic" bromine [8]. In aliphatic fluorocarbons, the replacement of halogen by hydrogen has also been reported by Miller [9].

2.1. Fluorinations with Halogen Fluorides

The procedures for hexachlorobenzene and pentachloro-α,α,α-trifluorotoluene were much alike throughout and are therefore described together. The hexachlorobenzene was a commercial product; the pentachloro-α,α,α-trifluorotoluene was a semiliquid slush or wet crystalline mass obtained by exhaustive chlorination of α,α,α-trifluorotoluene [10]. The bromine trifluoride was a commercial product, from several sources, used without purification.

The originally described procedure involved the slow addition of halocarbon to excess bromine trifluoride, in the cold in several portions, with intermittent heating to 100° C after addition of each portion. Two attempts to repeat the procedure led to destructive explosions in the later heating stages. Some of the associated patent specifications suggest other operating conditions [5]. A limited proportion of bromine trifluoride could be reacted smoothly with the halocarbon feed by adding the bromine trifluoride slowly to a stirred slurry of the halocarbon in liquid bromine.

Two forms of apparatus were used for different batch sizes. For batches of up to 500 g of halocarbon, the feed slurry was contained in a 500-ml nickel beaker in an ice bath, and stirred with a ⅛-hp stirrer. Bromine trifluoride was dripped in from a copper separatory funnel with a brass needle valve, in which the packing was replaced by Teflon and located on the downstream side, while the delivery tube was long and offset, to allow safe manipulation of the valve. Addition of bromine trifluoride usually required about 4 to 6 hr per batch. Operation was usually conducted outside the building when weather permitted, although in the laboratory a hood with good draft was sometimes used. Warm, humid weather was undesirable, as the condensation of water in the mixture led to waste of bromine trifluoride, excess heat, and accelerated corrosion. In equipment of this size, reaction began energetically and proceeded relatively smoothly until the addition of 1.6 to 1.8 moles of bromine trifluoride per mole of hexachlorobenzene or pentachloro-α,α,α-trifluorotoluene had been completed. After this point, reaction became very slow or ceased. A slight excess of bromine trifluoride appeared to remain unreacted after warming to 20° to 30° C and standing covered overnight.

Large batches (6 kg) of pentachloro-α,α,α-trifluorotoluene were fluorinated in a larger apparatus consisting of a welded Monel can of about 4-liter capacity with widened top to retain foam, a 15-gal ice bath, a 1-liter Monel separatory funnel, and a ¾-hp stirrer. This reaction vessel was monitored by a thermocouple and automatic recorder. The operator was shielded and remained at a distance, except for short trips to change valve settings or to

add ice to the bath. The course of reaction in this equipment was not quite consistent with observations in the smaller system. The temperature record on the chart was zigzagged, fluctuating between +10° and +80° C. An accumulation of bromine trifluoride in the cold alternated with a relatively rapid reaction (and temperature rise) which temporarily exhausted the bromine trifluoride and thus allowed the mixture to cool. Usually, the bromine trifluoride valve was turned off as soon as a sharp temperature rise began. When the flow was resumed before excessive cooling had ensued, accumulation of bromine trifluoride was lessened; and, with the best management, preparation of a large batch was completed in only 3 hr. Because of the great fluctuations observed, it is uncertain whether any of the large batches reached the same end point as the small batches.

There is a possibility that halogen replacement and chain-scission reactions could continue indefinitely, leading to CF_4 as the end product. However, carbon balances showed that loss of carbon in volatile form amounted, at most, to a very small percentage in the fluorination of pentachloro-α,α,α-trifluorotoluene, although it may have reached 8 percent with hexabromobenzene. It seems obvious that a large batch should not be started too cold, and that it would be quite hazardous to add very much bromine trifluoride until after the occurrence of some temperature rise that indicates the initiation of normal reaction.

Partial fluorinations were conducted upon some 30 small batches and 4 large batches involving, in all, 27 kg of pentachloro-α,α,α-trifluorotoluene, 4 kg of hexachlorobenzene, and 5 kg of hexabromobenzene. No explosions occurred in this stage, although the sharp rises in temperature observed with the large batches suggest that this might be possible with poor management. The character of products from this stage is shown in table 1. The analyses indicate that the present chlorofluoro intermediates, as obtained from this work, are less highly fluorinated and less saturated than those in the literature. It appeared desirable to saturate the materials to the highest possible extent, as any double bonds would lack fluorine atoms needed later, and would probably fail to take up fluorine in the exchange-fluorination step. Accordingly, the clear liquid products of the first step were mixed with more bromine trifluoride and heated to above 100° C, but with disappointing results.

Mixtures containing less than 10 to 15 percent by weight of bromine trifluoride, heated to 110° to 115° C for 6 hr, appeared to lose the fluorinating agent by evaporation, and the analysis and properties were unchanged. Mixtures containing 20 percent by weight of bromine trifluoride, heated to 120° to 130° C, appeared inert until a sudden explosive reaction occurred, vaporizing and spattering the product. In one instance, an explosion of material derived from hexachlorobenzene allowed about a 20 percent recovery of a clean, waxy, crystalline product, XII, probably similar to that mentioned in the literature [4]. Further high-temperature reactions were abandoned.

Other expedients found ineffective were the incorporation of small proportions of cobalt, lead, or manganese as possible catalysts, and, also, long exposure to fluorine gas at 25° C. When selected, high-boiling low-fluorine material derived from pentachloro-α,α,α-trifluorotoluene (II, V) was mixed with bromine trifluoride to form a clear solution, exposure to bright sunlight caused slow formation of bromine and evolution of heat. A low-boiling, high-fluorine fraction (III) did not react under the same conditions, although its analysis indicated some unsaturation. Chlorine trifluoride was able to react with these first-stage products (II). Bromine was evolved at first, and the mixture later became clear. The change in properties was, however, minor and the yield of fluoroaromatic products from a trial batch was not notably improved. An attempt to introduce chlorine trifluoride into cold, previously fluorinated material resulted in accumulation without reaction until an explosion destroyed the mixture. The method was not pursued further, despite its possible merits.

2.2. Hexafluorobenzene, Octafluorotoluene, and Some Chloro Derivatives

From the composition of intermediates quoted in the literature, it was hoped that the fluorinated materials could be dehalogenated without the intervention of an antimony pentafluoride reaction. When this step was omitted, however, the yield of product boiling under 145° C was nil; therefore antimony pentafluoride was used as prescribed. The reaction product was sometimes distilled to yield the rough fractions shown in tables 2 and 3, and was sometimes steam-distilled. A steam distillation residue, 40 percent by weight, yielded no useful low-boiling products upon subsequent dehalogenation.

TABLE 1. *Fluorination stages for pentachloro-α,α,α-trifluorotoluene*

Reaction	Fluorinating agent	Halocarbon	Product formula [a]	Weight	d_4^{24}	n_D^{24}
				g		
a	BrF_3, cold, 4,800 g	C_6Cl_5-CF_3, 5,600 g	$C_7Br_{0.6}Cl_{3.7}F_{7.0}$ Ha	7,600	2.00	1.4536
b	BrF_3, hot, 200 g	Ha,[b] 950 g	$C_7Br_{0.8}Cl_{3.2}F_{8.2}$ IIb	813	1.99	1.4532
c	SbF_5, 1,300 g	IIb,[c] 3,234 g	$C_7Br_{0.5}Cl_{2.5}F_{9.0}$	2,890	1.87	1.4186

[a] Average composition.
[b] Product from reaction (a).
[c] Product from reaction (b).

TABLE 2. *Fractions of fluorinated hexachlorobenzene after treatment with antimony pentafluoride*

Number	Boiling point	Weight	d_4^{20}	n_D^{24}	Gross composition			
					C	Br	Cl	F
	° C/mm	g						
XIII	50 to 90/7	1,427	1.87	1.4427	6	0.3	4.0	6.2
XIV	90 to 105/7	1,202	2.00	1.4749	6	.9	4.5	5.2
XV	105 to 115/7	200	.....	.....	6	1.2	4.7	6.0

TABLE 3. *Fractions of fluorinated pentachloro-α,α,α-trifluorotoluene after treatment with antimony pentafluoride*

Number	Boiling point	Weight	d_4^{24}	n_D^{24}	Gross composition			
					C	Br	Cl	F
	° C/mm	g						
III	25 to 70/10	2,490	1.836	1.4016	7	0.1	3.3	9.1
IV	71 to 80/10	1,430	1.882	1.4239	7	.4	3.7	8.5
V	60 to 115/2	1,347	1.998	1.4470	7	.8	3.9	7.8

Dehalogenation in ethanol was conducted as described in the literature [4]. Higher-boiling residues from this step were then dehalogenated in acetamide. The dehalogenation in ethanol furnished relatively pure perhaloaromatic compounds (VI, VII, XVII), but corresponding fractions from the acetamide operation were heavily contaminated with hydrogen compounds (VIII, IX), as indicated by mass spectra, higher refractive index, and lower density. Products of the two operations are compared in table 4. All of the octafluorotoluene was highly contaminated with heptafluorotoluene. The combined product apparently contained about 48 percent $C_6F_5CF_3$ and 50 percent $C_6F_4HCF_3$. Iodination of the mixture in fuming sulfuric acid converted the latter component into nearly pure 2-iodoheptafluorotoluene. The perfluorotoluene, which did not react, was subsequently hydrolyzed, yielding pentafluorobenzene.

TABLE 4. *Fluoroaromatic compounds from ethanol and acetamide dehalogenations*

Boiling range	Nominal formula	From ethanol		From acetamide		Identification
		d_4^{20}	n_D^{20}	d_4^{20}	n_D^{20}	
° C						
80 to 83	C_6F_6	1.628	1.3640	1.52	1.3704	XVI, XVIa
119 to 124	C_7ClF_5	1.672	.....	1.576	.....	XVII, XVIIa
102 to 111	C_7F_8	1.61	.....	1.50	.....	VI, VIII
138 to 139	C_7ClF_7	1.67	.....	1.58	.....	VII, IX

An examination of the chloroheptafluorotoluene by nuclear magnetic resonance, for which the authors are indebted to H. S. Gutowsky of the University of Illinois, indicated predominantly 2-chloroheptafluorotoluene with about 15 percent of another isomer, probably 4-chloroheptafluorotoluene.

The structure of the chloroheptafluorotoluene was further established as having the chlorine atom *ortho* [11] to the trifluoromethyl group by conversion to 1,2,3,4-tetrafluorobenzene. The *ortho* structure shows that fluorine atoms usually failed to add *ortho* to the trifluoromethyl group of the starting material, probably because of steric hindrance.

3. Experimental Procedure

3.1. Hexachlorobenzene and Bromine Trifluoride

A mixture of 100 g of hexachlorobenzene and 200 g of bromine was stirred in a 500-ml nickel beaker, surrounded by an ice bath. A supply of 264 g (1.92 moles) of bromine trifluoride was placed in a copper separatory funnel and about 50 g of this supply was dripped in slowly, with stirring, until the slurry had become nearly liquid. Further increments of hexachlorobenzene were added, followed by minor additions of bromine trifluoride, until a total of 285 g (1.00 mole) of hexafluorobenzene and about 150 g of bromine trifluoride had been added. The remaining bromine trifluoride was then slowly added. The total addition occupied 3 hr; stirring was continued overnight. Bromine and excess bromine trifluoride volatilized, leaving 340 g of a clear liquid, d_4^{25} 1.993.

Analysis: Found: C, 17.2; Br, 15.9; Cl, 40.6; F, 25.0.

3.2. Pentachloro-α,α,α-trifluorotoluene and Bromine Trifluoride (large batch)

In a Monel reactor having a 3.5—liter well and fitted with a ¾-hp stirrer was placed 5.72 kg (18.0 moles) of crude pentachloro-α,α,α-trifluorotoluene. From a large Monel separatory funnel, 4.3 kg (31.4 moles) of bromine trifluoride was added to the stirred halocarbon over a period of 6 hr. The reactor was surrounded by crushed ice in a 15-gal can. A distant thermocouple recorder showed temperature fluctuations between +10° and +50° C. The liquid product weighed 8.48 kg.

In the large-scale work with pentachloro-α,α,α-trifluorotoluene a total of 21.60 kg (67.7 moles) of pentachloro-α,α,α-trifluorotoluene and 15.54 kg (113 moles) of bromine trifluoride were reacted to yield 30.42 kg of fluorination product (II). Of this quantity, 28.5 kg was treated with 12.3 kg (57 moles) of antimony pentafluoride, giving a recovery of 20.2 kg of product (III–V). The product was dehalogenated with 16.1 kg of zinc in ethanol, the recovery being 12.38 kg of dehalogenated material, which yielded upon distillation 656 g (about 2.7 moles) of mixed polyflurotoluenes (VI), 4,895 kg (18.7 moles) of 2-chloro-α,α,α,3,4,5,6-heptafluorotoluene (VII), and 5.5 kg of residue. The smaller operations with 4 kg of hexachlorobenzene yielded about 25 g (about 1%) of crude hexafluorobenzene (XVI) and 307 g (about 12%) of chloropentafluorobenzene (XVII).

3.3. Hexabromobenzene and Bromine Trifluoride

In a 500-ml nickel beaker cooled in an ice bath were placed 138 g (0.25 mole) of hexabromobenzene and 100 ml of bromine. During 3 hr, a mixture of 53 g

(0.38 mole) of bromine trifluoride and an equal volume of bromine was added from a copper separatory funnel with stirring. The product (XIX) which formed during the addition weighed 62.5 g and consisted of clear, oily liquid and crystals. It distilled with decomposition at 200° to 250° C under atmospheric pressure, evolving large amounts of bromine. Partial distillation with less decomposition occurred at 1 to 2 mm.

Analysis: Calculated for $C_6Br_4F_6$: C, 14.2; Br, 63.2; F, 22.5. Found: Liquid—C, 14.1; Br, 63.6; F, 19.7. Crystals—C, 14.0; Br, 66.0; F, 17.7.

Another experiment used 552 g (1 mole) of hexabromobenzene and 274 g (2 moles) of bromine trifluoride. Half of the hexabromobenzene was put in the beaker, stirred with 300 g bromine, and one-quarter of the bromine trifluoride was added gradually, causing the mixture to become almost completely liquid. The remaining hexabromobenzene was then added, followed gradually by the remaining bromine trifluoride. The operation required 6 hr. After evaporation of volatile substances, the yield was 445 g of clear liquid, d_4^{25} 2.65. Table 5 gives a resume of these fluorination products (XIXa to d, XXVIII).

TABLE 5. *Fluorination of hexabromobenzene*

Agent	Mole ratio: Br F$_3$/ C$_6$Br$_6$	Yield	d_4^{24}	n_D^{24}	Gross composition			Identification
					C	Br	F	
		wt %						
BrF_3	3	56	2.58	1.4248	6	4.0	5.9	XIXa
BrF_3	1.5	45		1.4682	6	4.0	5.3	XIXb
BrF_3	2	82	2.65		6	4.0	3.5	XIXc
BrF_3	1.7	82	2.68	1.5342	...	...	...	XIXd
IF_5	0.5	~50	2.4	1.4913	6	3.3	6.1	XXVIII

[a] Fluorinating agent to hexabromobenzene.

3.4. Hexabromobenzene and Iodine Pentafluoride

In a Monel bomb of about 40-ml capacity, a mixture of 30 g (0.05 mole) of hexabromobenzene and 54 g (0.24 mole) of iodine pentafluoride was heated for 80 hr at 170° C. The product, after removal of iodine by thiosulfate, consisted of 18 g of mobile liquid (XXVIII), d_4^{25} 2.4, n_D^{20} 1.4913.

Analysis: Calculated for $C_6Br_4F_6$: C, 14.20; Br, 63.2; F, 22.5. Found: C, 15.4; Br, 56.4; F, 24.9. A larger batch consisting of 0.5 mole of C_6Br_6 and 0.5 mole of IF_5, heated under the same conditions, suddenly evolved bromine, causing the bomb to open and leaving a nearly stoichiometric residue of carbon. No reaction occurred at 96°.

3.5. Iodide Dehalogenations

To a solution of 515 g (3.4 moles) of sodium iodide in 1 liter of acetone in an Erlenmeyer flask was added 400 g of crude fluorination product (XIX) of density 2.65. The mixture was stoppered and left overnight with occasional shaking. After pouring onto ice and removing iodine with bisulfite and thiosulfate, the product was dried and distilled, yielding (XX) 13.5 g, bp 100°/35 mm, d_4^{25} 2.09, n_D^{24} 1.4426; molecular weight (in benzene), 380; (XXI) 185 g, bp 111° to 113° C/35 mm, d_4^{25} 2.39, n_D^{24} 1.4964, mp −15° to −17° C, molecular weight (in benzene), 420; (XXII) 59g, bp 95° to 100°/5 mm, d_4^{25} 2.56. Fraction (XXII) deposited crystals in the receiver. The analysis of (XXI) suggested that it might be impure $C_6Br_2F_6$. As a byproduct, a 660-g sample of fluorination product liberated 1 mole of iodine and no fluoride ions.

3.6. Acetamide Dehalogenation

To a three-necked flask containing 95 g of zinc dust and 20 g of sodium iodide in 300 g of acetamide at 100° C, 200 g of fraction XXI (preceding paragraph) was slowly added. The product, bp 83°, amounted to 50 g, had d_4^{25} 1.28 to 1.32, and showed the mass spectrometer peaks and ultraviolet absorption characteristics of impure 1,3,4-trifluorobenzene (XXVII).

3.7. Ethanol Dehalogenation

Absolute alcohol (700 ml) and 81.07 g of zinc dust were stirred in a large three-necked flask, and 310 g of fraction XXI was gradually added. The crude untreated products (XIX), from the reaction of a total of 4.5 kg (8.15 moles) of hexabromobenzene with bromine trifluoride, were processed likewise. The total product was fractionally distilled in a jacketed column. The principal fractions were (XXIII) 121.6 g (0.48 mole), $C_6H_2BrF_5$, bp 121° to 123° C, d_4^{25} 1.78, n_D^{25} 1.4080; (XXIV) 11.5 g (0.05 mole) impure $C_6H_2BrF_3$, bp 144° to 146°; (XXV) 225 g (about 0.70 mole) of a fraction mainly consisting of $C_6H_2Br_2F_4$ and $C_6Br_2F_6$, bp 164° to 169°/750 mm, 60° to 64°/10 mm, d_4^{25} 2.09, n_D^{25} 1.4565, mp −7.5°; and (XXVI) 20 g of higher-boiling material, bp 80° to 82°/10 mm, d_4^{25} 2.21. Fraction XXIV was identified by mass spectrometer.

Analysis: Found for XXIII: C, 28.5; H, 0.8; Br, 32.3; F, 38.3. Calculated for $C_6H_2BrF_5$: C, 28.9; H, 0.8; Br, 32.3; F, 38.2. Found for XXV: C, 21.0; H, 0.6; Br, 48.5; F, 28.6. Calculated for $C_6HBr_2F_5$: C, 22.0; H, 0.3; Br, 48.9; F, 29.0. Found for XXVI: C, 22.3; H, 0.4; Br, 55.6; F, 21.5.

3.8. Bromine Trifluoride and Chloranil

Chloranil, 123 g (0.5 mole), was stirred in a nickel beaker with 200 ml of bromine while being cooled in an ice bath. Bromine trifluoride, 100 g (0.75 mole), prediluted with 100 ml of bromine, was gradually dropped in over a period of 4 hr. The product, 130 g, was filtered to yield crystals and an oil. The crystals, after washing with ligroin and recrystallizing from methanol, melted at 64° to 65.5°. The oil distilled at 50° to 98° under 1 mm pressure, and had d_4^{25} 2.04. A small sample of the crystals, treated with zinc in ethanol and then oxidized with nitric acid, yielded trichloroquinone.

Analysis: Found for crystals: C, 21.0; Br, 23.7; Cl, 40.7; F, 5.9. Calculated for $C_6BrCl_4FO_2$: C, 20.8; Br, 23.2; Cl, 41.2; F, 5.5. Found for oil: C, 18.2; Br, 26.7; Cl, 32.5; F, 13.0. Calculated for $C_6BrCl_4F_3O_2$: C, 18.8; Br, 20.9; Cl, 37.0; F, 14.9.

4. References

[1] Y. Desirant, Bull. classe sci., Acad. roy. Belg. [5] **41,** 759 (1955).

[2] M. Hellmann, E. Peters. W. J. Pummer, and L. A. Wall, J. Am. Chem. Soc. **79,** 5654 (1957).

[3] J. A. Godsell, M. Stacey, and J. C. Tatlow, Nature **178,** 199 (1956).

[4] E. T. McBee, V. V. Lindgren, and W. B. Ligett, Ind. Eng. Chem. **39,** 378 (1947).

[5] E. T. McBee, V. V. Lindgren, and W. B. Ligett, U.S. Patents 2,461,554, Feb. 15, 1949; 2,471,831, May 31, 1949; 2,480,080, Aug. 23, 1949; 2,488,216, Nov. 15, 1949; 2,489,969, Nov. 29, 1949; and 2,498,891, Feb. 28, 1950.

[6] M. Hellmann, A. J. Bilbo, and W. J. Pummer, J. Am. Chem. Soc. **77,** 3650 (1955).

[7] B. Bak, D. Christensen, J. Rastrup-Andersen, Eileen Tannenbaum, and L. Hansen-Nygaard, J. Chem. Phys. **25,** 893 (1956); ibid. **26,** 135 (1957).

[8] T. van der Linden, Rec. trav. chim. **57,** 781 (1938).

[9] W. T. Miller, E. Bergman, and A. H. Fainberg, J. Am. Chem. Soc. **79,** 4159 (1957).

[10] E. T. McBee, J. S. Newcomer, W. E. Burt, and Z. D. Welch, Chapter on Preparation, properties, and technology of fluorine and organic fluorine compounds, Charles Slesser, ed., National Nuclear Energy Series, p. 783 (McGraw-Hill Publishers, New York, N.Y.).

[11] W. J. Pummer, R. E. Florin, and L. A. Wall, J Research NBS **62,** (1959) RP2939.

WASHINGTON, June 20, 1958.

Journal of Research of the National Bureau of Standards Vol. 62, No. 3, March 1959 Research Paper 2939

Synthesis of Some Disubstituted 3,4,5,6,-Tetrafluorobenzenes[1,2]

Walter J. Pummer, Roland E. Florin, and Leo A. Wall

The preparation of 1,2,3,4-tetrafluorobenzene from 2-chloroheptafluorotoluene in a two-step synthesis is described. A new method for the hydrolysis of the trifluoromethyl group was developed using alumina and steam at high temperatures. The products obtained from the hydrolysis of 2-chloroheptafluorotoluene were 2-chloro-3,4,5,6-tetrafluorobenzoyl fluoride and 2,3,4,5-tetrafluorochlorobenzene, the decarboxylated product. The latter compound was converted to 1,2,3,4-tetrafluorobenzene by reduction with hydrogen and palladium at 280° C and atmospheric pressure. Some of the new compounds prepared, in addition to those mentioned previously, include 2-chloro-3,4,5,6-tetrafluorobenzoic acid, 2-chloro-3,4,5,6-tetrafluoroiodobenzene, and 1,2-diiodo-3,4,5,6-tetrafluorobenzene.

1. Introduction

Recently the preparation of a perfluoropolyphenyl by the condensation of 1,4-diiodo-2,3,5,6-tetrafluorobenzene with activated copper [1][3] was reported. Since the synthesis of the precursor, 1,2,4,5-tetrafluorobenzene [2] was a tedious process, consideration was given to the possibility of converting a highly fluorinated toluene derivative into a tetrafluorobenzene, with the anticipation that the symmetrical isomer would be obtained. On the basis of availability, chloroheptafluorotoluene was chosen as the starting material. This compound, obtained as a byproduct from the synthesis of perfluorotoluene [4], was first reported by McBee [3]. No structure was assigned to the chloroheptafluorotoluenes. As it will be shown subsequently, this compound is predominantly the ortho isomer, i.e., 2-chloroheptafluorotoluene (I), with small amounts of the para isomer (II) present. None of the meta isomer (III) was observed.

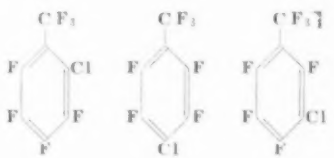

I II III

All the compounds obtained from the synthesis beginning with these materials were new and hitherto unknown. Since rearrangements were unlikely to occur during the reactions, characterization of the final tetrafluorobenzene as the 1,2,3,4-isomer established the fact that the chlorine atom was adjacent to the trifluoromethyl group in I and that it occupied the 2-position in the resulting compounds, IV to VIII. The reactions that were investigated (see scheme below), such as hydrolysis, decarboxylations, and reductions, also serve to illustrate some generally applicable methods of synthesis in the aromatic fluorocarbon series.

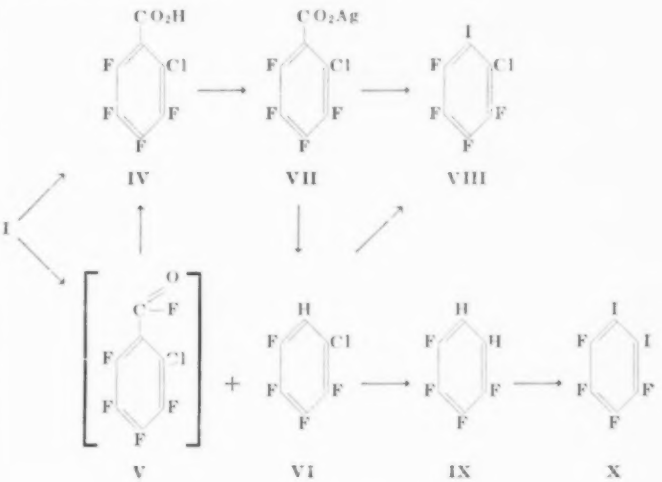

IV VII VIII

V VI IX X

2. Results

2.1. Hydrolysis of the Trifluoromethyl Group

Methods for this type of reaction have been described for benzotrifluoride [5] and perfluorotoluene [6]. The best results were obtained by prolonged refluxing with concentrated sulfuric acid. This technique was adapted to the hydrolysis of 2-chloroheptafluorotoluene (I) and gave a 49-percent yield of 2-chloro-3,4,5,6-tetrafluorobenzoic acid (IV).

In the search for improvement a new method was developed which involved the vapor-phase hydrolysis of I by the use of alumina and steam at high temperatures. The products of the reaction were 2-chloro-3,4,5,6-tetrafluorobenzoyl fluoride (V) and 2,3,4,5-tetrafluorochlorobenzene (VI), the decarboxylated product. The former was recovered by extraction with dilute potassium hydroxide and later acidified to yield (IV), while the latter was obtained by distillation of the residual liquid. The recovered

[1] This paper is based on work sponsored by the Ordnance Corps, Department of the Army, Washington, D.C.

[2] Presented as part of the Symposium on Fluorine Chemistry, Division of Industrial and Engineering Chemistry, at the 134th Meeting of the American Chemical Society, Chicago, Illinois, September 1958.

[3] Figures in brackets indicate the literature references at the end of this paper.

2-chloroheptafluorotoluene (I) could then be recycled. This reaction was studied at different temperatures, in atmospheres of wet and dry nitrogen, and with different grades of alumina. Maximum conversion was obtained at 330° C. The results are shown in table 1.

The first example shows the results obtained at a lower temperature and in the absence of added moisture. However, there was sufficient water vapor remaining on the alumina to cause hydrolysis but not decarboxylation. Once the water was removed, the reaction stopped, as evidence by the high recovery of (I). With water-pumped nitrogen, i.e., by introducing traces of water, some decarboxylation occurred. The Pyrex glass furnace tube was eventually replaced by a copper tube because occasionally ring fluorine was removed by the reaction of the wet fluorocarbon with glass. This action was eliminated by the use of the copper tube.

Of special interest were the results obtained with the pellet-size alumina. At a slow input rate, a 60 percent conversion to 2,3,4,5-tetrafluorochlorobenzene (VI) was obtained. Then, by increasing the rate, i.e., increasing the nitrogen flow and raising the temperature of the vaporizer, it was possible to increase the relative yield of 2-chloro-3,4,5,6-tetrafluorobenzoyl fluoride (V). This was not surprising, however, since at the slow rate, V was in the furnace longer and hence it had more time to form a complex with the alumina, which in the presence of steam was decarboxylated. At the fast rate, then, the time in the furnace was decreased thereby reducing complex formation. The 8–14 mesh alumina had about the same activity as the pellets. The pellets were more effective than the powder-trail technique, mainly because the vapor had to pass through the reagent, resulting in better contact for reaction to occur.

An attempt was made to elucidate the mechanism by which 2,3,4,5-tetrafluorochlorobenzene (VI) was formed. This could occur either by direct removal of the trifluoromethyl as trifluoromethane or by the hydrolysis of this group, followed by decarboxylation. In one experiment, the effluent gases were collected in a liquid-nitrogen trap and analyzed in the mass spectrometer. The gas sample contained 99.6 percent of carbon dioxide, which confirms the hydrolytic mechanism.

2.2. Replacement Reactions

Several methods of replacing the carboxyl group, in the form of salts that were used so successfully by Hazeldine [7], La Zerte [8], and Henne [9] for the perfluoroaliphatic acids, have been extended to the 2-chloro-3,4,5,6-tetrafluorobenzoic acid (IV).

When an intimate mixture of silver-2-chloro-3,4,5,6-tetrafluorobenzoate (VII) and excess iodine were pyrolyzed, a 16 percent yield of 2-chloro-3,4,5,6-tetrafluoroiodobenzene (VIII) was obtained, along with an unidentified high-boiling residue (probably a coupling product). La Zerte [8] reported that silver-perfluorocaprylate undergoes a coupling reaction in 77 percent yield to $C_{14}F_{30}$. A similar reaction may be occurring with the salt VII.

An alternate route to VIII has been accomplished by an indirect approach. The decarboxylation of the silver salt VII in ethylene glycol at 170° C for 1 hr produced an 87-percent yield of the same 2,3,4,5-tetrafluorochlorobenzene (VI) that was obtained from the alumina hydrolysis reaction above. The high yield of the hydrogen compound (VI) rivals those obtained by La Zerte [8] for the aliphatic fluorocarbon hydrides. Iodination of VI in 65 percent oleum gave a 67-percent yield of 2-chloro-3,4,5,6-tetrafluoroiodobenzene (VIII).

a. Reduction

In order to obtain the tetrafluorobenzene (IX) from 2,3,4,5-tetrafluorochlorobenzene (VI), it was necessary to remove the chlorine preferentially without the elimination of any fluorine. This problem was solved neatly by passing the vaporized chloro compound VI together with hydrogen gas through a catalyst composed of 10 percent palladium mounted on activated ⅛ in. charcoal pellets at 280° C. The chlorine was removed predominantly in 70- to 90-percent yields with less than 1 percent of the fluorine eliminated. This reduction reaction should find great use as a tool in synthesis in aromatic fluorocarbon chemistry. Thus the relative ease by which 1,2,3,4-tetrafluorobenzene (IX) can be obtained from 2-chloroheptafluorotoluene (I) in a simple two-step synthesis (I→ VI→ IX) has been demonstrated.

TABLE 1. *Hydrolysis of* $C_6F_4ClCF_3$ (I) *over alumina*

Weight of compound	Catalyst size	Tube material	N_2 flow	Vaporizer temperature	Furnace temperature	Recovered $C_6F_4ClCF_3$	Conversion		Total time
							C_6F_4ClCOF (I)	C_6F_4ClH (VI)	
g	*Mesh*		*cm³/min*	*° C*	*° C*	*%*	*%*	*%*	*hr*
200	[a] 80 to 200	Pyrex	[d] 125	110	324	81.6	63	0	13
100	[a] 80 to 200	do	[e] 125	108	335	33.1	33.1	13.8	5.5
966	[a] 80 to 200	Copper	[f] 125	110	330	49.4	17.5	34.8	33
549	[b] ⅛ in. pellets	do	[f] 200	120	330	48.9	67.1	24.7	12
1000	do	do	[f] 125	110	330	63.2	22.7	60.1	35
1073	[c] 8 to 14	do	[f] 125	110	330	67.1	21.8	59.6	36

[a] Merck chromatographic grade. Powder trail on the bottom of the tube.
[b] Harshaw Puralox. Completely filled.
[c] Fisher Scientific. Completely filled.
[d] Prepurified nitrogen with no moisture added.
[e] Water-pumped nitrogen containing traces of water.
[f] Prepurified nitrogen saturated with water.

3. Discussion

The tetrafluorobenzene (IX) prepared by the above route has a boiling point of 95° C. A mass spectrometer analysis of a fractionated sample showed no observable impurities. Finger [10] stated that the 1,2,3,4-tetrafluorobenzene (IX) prepared by a different method has a boiling point slightly lower than 95° C. The other two isomers, the 1,2,4,5-[2] and the 1,2,3,5-[11] tetrafluorobenzenes, have boiling points of 88° and 83° C, respectively. Furthermore, the nuclear magnetic resonance spectra of IX, obtained by Prof. H. S. Gutowsky at the University of Illinois, have shown conclusively that the two hydrogen atoms are adjacent to one another. Also, this tetrafluorobenzene (IX) was iodinated to a new 1,2-diiodo-3,4,5,6-tetrafluorobenzene (X), mp 50.8° to 51.5° C. Previously the 1,4-diiodo-2,3,5,6-tetrafluorobenzene, mp 109° to 111° C, [1] was prepared in this laboratory. The 1,3-diiodo-2,4,5,6-tetrafluorobenzene is at present unknown. However, the existence of this product was eliminated as a possibility because of the boiling point of the precursor IX. Therefore, on the basis of its boiling point, nuclear magnetic resonance pattern, and iodinated product (X), it is shown that the tetrafluorobenzene (IX) is, indeed, the 1,2,3,4-isomer. Since this compound (IX) was prepared in considerable quantity from a chloroheptafluorotoluene of unknown isomerism, the 2-chloroheptafluorotoluene structure is assigned to (I).

A small fraction (less than 3%) of a tetrafluorobenzene, boiling point 88° to 90° C, contaminated with a trifluorobenzene of unknown structure was obtained as a byproduct. On the basis of its boiling point it was tentatively assigned the known 1,2,4,5-tetrafluorobenzene structure. This compound could have been obtained only from small amounts of the 4-chloroheptafluorotoluene (II) present in the original material.

The presence of a sizable amount of (I) among the many products obtained from the synthesis of perfluorotoluene [3, 4], can readily be accounted for by assuming that the fluorination conditions were not drastic enough to overcome the steric effects of the trifluoromethyl group. This resulted in failure to saturate the double bond adjacent to the trifluoromethyl group with fluorine, thereby leaving an unreactive chlorine atom in the molecule which could not be removed by zinc dehalogenation.

4. Experimental Procedure [4]

4.1. Hydrolysis of 2-Chloroheptafluorotoluene I

a. Sulfuric Acid Method

2-Chloroheptafluorotoluene (I), 270 g (1.07 moles), was hydrolyzed to 2-chloro-3,4,5,6-tetrafluorobenzoic acid (IV) (120 g, 49.2% yield, mp 83° to 88° C) by McBee's method [5] for perfluorotoluene, except that only 48 hr were required. Evolution of HF during this period was fair. One recrystallization from a ligroin-toluene mixture, followed by sublimation at 80° C/10 mm afforded white plates, mp 89° to 91° C.

Analysis: Calculated for $C_7HClF_4O_2$: C, 36.79; H, 0.44; Cl, 15.51; F, 33.25. Found: C, 36.2; H, 0.31; Cl, 15.70; F, 32.8.

The anilide derivative was prepared in the usual fashion, and after several recrystallizations from aqueous alcohol yielded white leaflets, mp 207° to 208.5° C.

Analysis: Calculated for $C_{13}H_6ClF_4NO$: N, 4.61; Cl,11.67. Found: N, 4.40; Cl, 12.10.

b. Alumina Method

The apparatus consisted of a 500-ml round-bottom flask, which served as the vaporizer, with a side arm attached to a horizontally mounted copper tube furnace (30 in. long, 1⅛ in. diam) by means of a 14/20-mm ball-and-socket joint. The outlet of the furnace was connected to a 500-ml round-bottom receiver containing a stopcock at the bottom for drainage. The vaporizer was fitted with a 24/40-mm through-joint and the lower portion extended almost to the bottom of the flask. The upper end of this joint was Y-shaped. One side was used for filling the vaporizer, while the other side was connected to a gas dispersion trap containing 400 ml of water from which the nitrogen acquired its moisture.

In a typical run, when the furnace had reached the desired temperature (330° C), 1 kg of 2-chloroheptafluorotoluene (I) was placed in the vaporizer maintained at 120° C. It was carried into the furnace by the aid of the wet nitrogen. The rate was controlled by the nitrogen flow and the temperature of the vaporizer bath. The products (899 g) were collected in the receiver maintained at room temperature. They were shaken with three 200-ml portions of 10 percent potassium hydroxide to remove the 2-chloro-3,4,5,6-tetrafluorobenzoyl fluoride (V) as the potassium salt of the acid (IV). Acidification of the combined basic solutions afforded 85 g (22.7% conversion, based on reacted I) of 2-chloro-3,4,5,6-tetrafluorobenzoic acid (IV), mp 88° to 90° C. The base insoluble liquid was washed with 500 ml of water, dried (Na_2SO_4), and distilled. There was obtained 161 g (60%, based on reacted I) of 2,3,4,5-tetrafluorochlorobenzene (V), boiling point 121.5° to 123° C; $n_D^{20} = 1.4391$; $D_{24}^{24} = 1.534$.

Analysis: Calculated for C_6HClF_4: H, 0.54; Cl, 19.21. Found: H, 0.50; Cl, 18.90. The recovered 2-chloroheptafluorobenzene, 632 g, was then recycled.

The crude acid fluoride V (boiling point 161° to 164° C) reacted readily with cold concentrated ammonium hydroxide to form the 2-chloro-3,4,5,6-tetrafluorobenzamide, mp 101° to 103° C after two recrystallizations from 50 percent ethanol.

Analysis: Calculated for $C_7H_2ClF_4NO$: C, 36.9; Cl, 15.6; F, 33.4; N, 6.15. Found: C, 36.9; Cl, 15.7; F, 34.0; N, 6.1.

[4] Boiling points and melting points are not corrected. Chemical analyses were performed by Messrs. Paulson and Machlan, and mass spectrometer analyses by Miss Edith Quinn.

4.2. Silver-2-Chloro-3,4,5,6-Tetrafluorobenzoate (VII)

Fifty grams (0.22 mole) of the acid IV was dissolved in excess dilute NH_4OH. When the excess ammonia was removed by boiling, a solution of 50 g (0.30 mole) of silver nitrate in 75 ml of water was added with stirring. The mixture was cooled, and the silver salt (VII) was collected by filtration. After washing with 60 ml of cold distilled water, 50 ml of cold methanol, and 100 ml of petroleum ether, the salt (VII) was dried in an oven at 110° C for 72 hr and then for 24 hr more over Drierite. The dried silver salt (VII) weighed 60.5 g; 82-percent yield.

4.3. 2-Chloro-3,4,5,6-Tetrafluoroiodobenzene (VIII)

a. Direct Method

Into a 250-ml round-bottom flask was placed an intimate mixture of 30 g (0.09 mole) of silver-2-chloro-3,4,5,6-tetrafluorobenzoate (VII) and 90 g (0.35 mole) of iodine. The flask was fitted with a reflux condenser which was attached to a solid carbon dioxide trap leading to a mineral-oil bubbler. The reaction was initiated by gently heating the upper edges with a Bunsen burner. The heating was gradually applied around the flask and continued until the reaction ceased. The flask was cooled, and the contents extracted several times with ether. The combined ether solutions were successively washed with 50-ml portions of 10 percent sodium bisulfite, 10 percent sodium carbonate, water, 10 percent hydrochloric acid, water, and finally dirzd over anhydrous calcium chloride. After removal of the solvent and distillation of the residue, there was obtained 4.5 g (16.2% yield) of 2-chloro-3,4,5,6-tetrafluoroiodobenzene (VIII), boiling point 71° to 72° C/6 mm; $n_D^{20}=1.5349$.

Analysis: Calculated for C_6F_4ClI: C, 23.21; F, 24.50; I, 40.83. Found: C, 23.20; F, 24.50; I, 41.95. There was obtained also 2 g of a high-boiling residue (150° to 200° C/1 mm) which has not been identified, but may possibly be a coupling product.

b. Indirect Method

First Step: 2,3,4,5-Tetrafluorochlorobenzene (VI). Thirty grams (0.09 mole) of the silver salt (VII) and 15 g of ethylene glycol were placed into a 250-ml flask, fitted with a reflux condenser leading to a solid carbon dioxide trap. The flask was inserted gradually into a Wood's-metal bath at 160° C. Marked refluxing of the product was evident after about 10 min., and the reaction appeared to be complete after 20 min. However, to insure completion, the temperature was slowly raised to 170° C for 1 hr more. The mixture was cooled to below 100° C and the apparatus rearranged for distillation. The 2,3,4,5-tetrafluorochlorobenzene (VI) distilled at 122° to 123° C, weight 14.3 g (86.5% yield); $D_{24}^{24}=1.536$: $n_D^{20}=1.4396$.

Second step: Into a 100-ml three-necked flask, fitted with a stirrer, dropping funnel, and reflux condenser, were placed 13 g (0.05 mole) of iodine and 15 ml of 65 percent fuming sulfuric acid. To the stirred reaction mixture was added 6 g (0.0325 mole) of 2,3,4,5-tetrafluorochlorobenzene (VI) dropwise over a ½-hr period. When the addition was completed, the stirred mixture was heated at 60° C in a water bath for 2 hr. The reaction mixture was cooled, poured onto 50 g of ice, and decolorized by the addition of 100 ml of 10 percent aqueous sodium bisulfite. An ether extraction, followed by drying (Na_2SO_4) and distillation, afforded 6.83 g (66.9% yield) of 2-chloro- 3, 4, 5, 6-tetrafluoroiodobenzene (VIII), boiling point 70° to 72° C/5 mm.

4.4. 1,2,3,4-Tetrafluorobenzene

For the reduction of 2,3,4,5-tetrafluorochlorobenzene (VI) the same apparatus was used as described above for the alumina method of hydrolysis, except that the furnace tube was made of 20 mm Pyrex tubing and only a 5-in. section contained the catalyst. The gas dispersion trap contained concentrated sulfuric acid, instead of water, for drying the hydrogen. Twenty grams of the moist catalyst (10% palladium on ⅛ in. activated charcoal pellets)[5] were placed in the furnace and preheated at 280° C for 2 hr in the hydrogen atmosphere. When the water was removed, 123 g (0.66 mole) of VI was placed in the vaporizer maintained at 110° C. The hydrogen flow rate was adjusted to 100 cm^3/min, and 4 hr were required to complete the run. The products (97 g.) were washed with three 100 ml portions of water, dried (Na_2SO_4), and distilled. There was obtained 77.2 g (77% yield) of 1,2,3,4-tetrafluorobenzene (IX); boiling point 94.8–95° C; $n_D^{20.2}=1.4095$; $D_{23.5}^{23.5}=1.401$. No impurities were observed from the mass spectrometer analysis.

Analysis: Calculated for $C_6H_2F_4$: C, 48.0; H, 1.3. Found: C, 48.4; H, 1.4.

There was also obtained a small forerun, 3 g., boiling point 88° to 90° C; from the mass spectrometer analysis it was found to be a mixture of 60 percent tetrafluorobenzene (presumably the 1,2,4,5-isomer) and 40 percent trifluorobenzene of unknown structure. These products were not further investigated.

4.5. 1,2-Diiodo-3,4,5,6-Tetrafluorobenzene (X)

The iodination of 1,2,3,4-tetrafluorobenzene (IX) was performed by the same procedure as described for the 1,2,4,5-isomer [1] except that the following quantities were used: 250 g (1.66 moles) of IX 454

[5] Columbian grade, 4 to 6 mesh, CXAL, activated carbon, Carbide and Carbon Company.

g (1.79 moles) iodine, and 1.3 kg 65 percent fuming sulfuric acid. The 1,2-diiodo-3,4,5,6-tetrafluorobenzene (X) obtained after recrystallization from 60 percent ethanol-water mixture weighed 455 g, 67-percent yield, mp 50.5° to 51.8° C (white plates).

Analysis: Calculated for $C_6F_4I_2$: I, 63.1. Found: I, 62.3.

The authors thank H. S. Gutowsky of the University of Illinois for performing and interpreting the nuclear magnetic resonance analysis of the 1,2,3,4-tetrafluorobenzene. We also express our appreciation to Gilbert Gavlin, The Richardson Company, for helpful discussions concerning the use of alumina for the hydrolysis reaction.

WASHINGTON, February 19, 1958.

5. References

[1] M. Hellmann, A. J. Bilbo, and W. J. Pummer, J. Am. Chem. Soc. **77,** 3650 (1955).
[2] G. C. Finger, F. H. Reed, D. M. Burness, D. M. Fort, and R. R. Blough, J. Am. Chem. Soc. **73,** 145 (1951).
[3] E. T. McBee, V. V. Lindgren, and W. B. Ligett, Ind. Eng. Chem. **39,** 379 (1947).
[4] R. E. Florin, W. J. Pummer, and L. A. Wall, J. Research NBS **62,** (1959) RP2938.
[5] G. M. LeFave, J. Am. Chem. Soc. **71,** 4148 (1949).
[6] E. T. McBee and E. Rapkin, J. Am. Chem. Soc. **73,** 1366 (1951).
[7] R. N. Hazeldine, J. Chem. Soc. **1951,** 584.
[8] J. D. La Zerte, L. J. Hals, T. S. Reid, and G. H. Smith, J. Am. Chem. Soc. **75,** 4525 (1953).
[9] I. Auerbach, F. H. Verhoek, and A. L. Henne, J. Am. Chem. Soc. **72,** 299 (1950).
[10] G. C. Finger, R. E. Oesterling, and R. H. White, paper presented before the Division of Organic Chemistry at 130th Meeting of the American Chemical Society, Atlantic City, N.J., September 1956.
[11] G. C. Finger, F. H. Reed, and R. E. Oesterling, J. Am. Chem. Soc. **73,** 152 (1951).

Journal of Research of the National Bureau of Standards Vol. 62, No. 3, March 1959 Research Paper 2940

Reactions of Aromatic Fluorocarbons with Hydrogen[1, 2]

Roland E. Florin, Walter J. Pummer, and Leo A. Wall

Various palladium and platinum catalysts were used to effect the following hydrogenation reactions at relatively high conversions and yields:

$$C_6F_4ClH \xrightarrow[280°]{Pd} C_6F_4H_2$$

$$C_6F_4ClCF_3 \xrightarrow[280°]{Pd} C_6F_4HCF_3$$

$$C_6F_6 \xrightarrow[300°]{Pt} C_6F_5H,\ C_6F_4H_2$$

Nickel could be used for some of the reactions, but with much greater difficulty. The products of these reactions can be iodinated and brominated, and hence are a starting point for the synthesis of many new derivatives of aromatic fluorocarbons.

1. Introduction

Derivatives of aromatic fluorocarbons with one and two reactive functional groups are desirable for the synthesis of high-temperature-resistant polymers. The mono- and dihydro-derivatives, e.g., pentafluorobenzene and tetrafluorobenzene, can be readily brominated and iodinated to form iodopentafluorobenzene and diiodotetrafluorobenzene, which are desirable starting substances for further syntheses.

It has now been found possible to prepare the requisite hydrogen compounds by a high-temperature hydrogenation of the more readily available perfluoro and chlorofluoro aromatics. Many common procedures for hydrogenation, when applied to haloaromatics, encounter difficulty due to catalyst poisoning; others often lead to saturation of the molecule to form the cyclohexane ring. However, nickel at high temperatures and atmospheric pressure will remove chlorine without becoming poisoned and without saturating the ring [1];[3] more recently it has been found that molybdenum disulfide at about 500° C can act likewise [2].

When Swarts [3] tried to use nickel at 270° C for the hydrogenation of fluorobenzene he was unable to proceed because of rapid poisoning of the catalyst. Low-temperature hydrogenation upon platinum was very rapid, as the catalyst was immune to poisoning by hydrogen fluoride or silicon tetrafluoride. Unfortunately, fluorobenzene formed cyclohexane exclusively without a trace of benzene.

2. Results and Discussion

The present procedure is essentially a Sabatier method, but employs various catalysts. It was found possible to use nickel in the reduction of chloropentafluorobenzene, chlorotetrafluorobenzene, and chloroheptafluorotoluene to produce moderate yields of tetrafluorobenzene and heptafluorotoluene, but low activity and fairly rapid poisoning made the operation difficult. The most useful form of nickel appeared to be a thin layer of powder along the bottom of the furnace tube. The relative amounts of chloride and fluoride liberated varied with the type and age of the nickel catalyst. Spent catalyst could be regenerated partially by passage of water vapor, but the restored activity did not last long. The distillation behavior of both the trerafluorobenzene and the heptafluorotoluene suggests the presence of several isomers.

By contrast, catalysts of palladium on carbon and platinum on carbon were efficient and durable, permitting many successive runs and high conversions per pass. Palladium was highly selective for chlorine removal at 280° C. At 300° C and in the presence of moisture it also effected the removal of fluorine from hexafluorobenzene, but soon lost its activity, possibly by sintering. Platinum at 300° C removed fluorine from hexafluorobenzene, and retained its activity for long times. The yield of monohydro derivative was high. At 17 percent conversion of hexafluorobenzene over palladium, the distribution of products was 40 percent pentafluorobenzene, 10 percent tetrafluorobenzenes, and 4 percent trifluorobenzenes. Product distributions using platinum catalyst at conversions up to 58 percent appear roughly similar. The large proportions of monohydro derivatives seem contrary to the implications of classical work on other polyhalogenated benzenes [1], for which it is stated that the fewer the remaining halogens, the more easily the reduction proceeds.

A few further points call for brief discussion. (1) The importance of high temperatures for substitution without saturation has an obvious, though not strictly necessary, connection with the benzene-cyclohexane equilibrium, which becomes rather favorable to benzene around 300° C. (2) The reason for the selectivity of palladium for chlorine is obscure. Possibly in the surface-activated complex the palladium has a preferential attraction for the

[1] Presented as part of the Symposium on Fluorine Chemistry, Division of Industrial and Engineering Chemistry, at the 134th Meeting of the American Chemical Society, Chicago, Ill., September 1958.

[2] This work was performed as part of a research project sponsored by the Bureau of Aeronautics, Department of the Navy, Washington 25, D.C.

[3] Figures in brackets indicate the literature references at the end of this paper.

chlorine atom, weakening the carbon-chlorine bond. The neighboring element, silver, appears to have a strong affinity for chlorine relative to fluorine, as indicated by solubilities of the halides [4]. (3) Hydrogenation attacks the ring halogen and leaves the trifluoromethyl group untouched, while the reverse is true for hydrolysis over alumina [5].

It is tempting to extend as far as possible the familiar classifications of solution chemistry. Steam on alumina is probably essentially an acid reagent. Hydrogen on noble metals may stand between the pure free-radical and pure basic reagents, with more free-radical character on palladium and more basic character on platinum. Basic reagents attack ring halogens fairly readily, sometimes observing the usual order of reactivity I>Br>Cl>F, and sometimes reversing the order [6]. Further studies with hydrogen involving other halogenated aromatic compounds would be desirable.

3. Experimental Procedures

3.1. Apparatus and Method

Most of the hydrogenations were conducted in a train consisting of hydrogen tank, flowmeter, water or concentrated sulfuric acid bubbler, vaporizing flask, furnace tube, receiver, solid carbon dioxide trap, and water bubbler. In most experiments the hydrogen was dried, but occasionally water was deliberately introduced. The vaporizing flask was held at a temperature 5° to 20° C below the boiling point of the halogen compound to be used in order to furnish a convenient partial pressure of the compound. Connections from it to the furnace tube were heated by windings of resistance wire or commercial heating tape to avoid condensation. A ball joint sealed with polychlorotrifluoroethylene grease was a convenient joint at this location. The furnace tube and subsequent parts were made of glass or copper. Glass parts were usually convenient and did not seem to interfere with the reaction in any case, but when large amounts of hydrogen fluoride were liberated the reactors were often perforated before the end of a single run and the final water bubbler was always rapidly clogged with silica derived from hydrolysis of silicon tetrafluoride. Therefore, in large-scale work involving liberation of hydrogen fluoride the furnace tube and receiver were of copper. Clogging of the final water bubbler with silica was also lessened by discharging the gas into water through an underlying layer of carbon tetrachloride. Products from the receiver were washed with water, dried, distilled, and analyzed by density, refractive index, and mass spectrometry. When hexafluorobenzene was being converted to pentafluorobenzene and other fluorinated benzenes, it was convenient to iodinate the products [7] before attempting distillation.

For hydrogen halide determinations the water washings from receiver, cold trap, and water bubbler were combined and a diluted aliquot taken. Chloride was determined by the Mohr titration, and fluoride by the thorium titration with alizarin indicator [8].

3.2. Catalysts

The only useful form of nickel was the commercial reagent grade powder. Unsuccessful forms included the powder mixed with glass wool; a nickel on charcoal catalyst made by soaking the charcoal in nickel nitrate, heating, and reducing; similar preparations on alumina; and also preparations on reduced copper oxide wire. The inactivity of the copper-supported catalyst was to be expected in view of well-known studies on the mechanism of catalysis. Further unsuccessful catalysts included copper, as reduced copper oxide wire, and molybdenum sulfide prepared according to Lazier [2].

Palladium on carbon was prepared by dissolving 5 g of palladium in aqua regia, evaporating twice with concentrated hydrochloric acid, diluting with water, pouring over 25 g active carbon,[4] and heating with alkaline formaldehyde. The product was stored wet. Platinum on carbon was prepared in the same way, but starting from commercial chloroplatinic acid. All catalysts were reduced for several hours before using.

3.3. Chloropentafluorobenzene Over Nickel

The chloropentafluorobenzene consisted of several samples, boiled at 120° to 125° C, d_4^{26} 1.54 to 1.57, n_D^{26} 1.4189 to 1.4355, obtained from the preparation of hexafluorobenzene [9, 10]. Using the general apparatus described, 24.7 g of chloropentafluorobenzene was placed in the vaporizer at 100° C and passed through a 2- by 60-cm furnace tube containing about 100 g of nickel powder in a thin layer, over a period of 3.7 hr. The collected product contained 4.48 g impure tetrafluorobenzene, boiled at 88° to 91° C, d_4^{24} 1.39, n_D^{24} 1.4105, and 14.3 g recovered feed. Mass spectra indicated about 75 percent tetrafluorobenzene and 25 percent trifluorobenzene in the low-boiling fraction. The ultraviolet absorption was similar to that of known 1,2,4,5-tetrafluorobenzenes, but ultraviolet spectra do not discriminate well between the positional isomers. The low-boiling fraction probably contained the 1,2,3,5 and 1,2,4,5 isomers, but little of the 1,2,3,4 isomer, which is known to boil at 95° C [5]. Subsequent experiments produced also fractions boiling in the range 92° to 98° C, now believed to have contained 1,2,3,4-tetrafluorobenzene. After several recyclings, the chloropentafluorobenzene fraction became lower in density. It is likely that fluorine removal had occurred to produce chlorotetrafluorobenzene.

[4] Columbia CXAL, 4 to 8 mesh, low in copper and ash, obtained from Carbide and Carbon Chemicals Co.

3.4. Chloroheptafluorotoluene Over Nickel

The 2-chloroheptafluorotoluene was a by-product of the preparation of perfluorotoluene [9, 10]. Arrangements were as in the preceding example, except that the vaporizer bath temperature was kept at 115° C and the furnace temperature at 258° to 285° C. In many runs, a total of 1,099 g (4.36 moles) of chloroheptafluorotoluene yielded 85 g (0.39 mole) of somewhat impure heptafluorotoluene, $C_6F_4HCF_3$, boiled at 103° to 112° C, 0.49 equivalents of chloride and 0.15 equivalents of fluoride in wash waters, and 877 g (3.44 moles) of starting material. The aggregate time was 60 hr. The product contained several incompletely separated fractions, the larger of which are shown in table 1. The slow decline of catalyst activity is shown in table 2. Regeneration with water vapor was effective but only for a short time. Other arrangements of the nickel were inferior. Mixing with glass wool throughout the volume of the tube resulted in very little reaction. Attempts to pass vapor upward through a bed of powder gave poor conversions and rapid plugging. Nickel on charcoal, packed into the tube, produced an initial heavy burst of chloride and fluoride liberation, followed by inactivity. No changes were found in the properties of recovered feed materials.

TABLE 1. *Reduction products of chloroheptafluorotoluene*

Boiling point	Weight	Density	Refractive index
°C	g	d_4^{24}	n_D^{22}
101 to 104	31.6	1.532 to 1.536	1.3753 to 1.3779
105 to 108	15.0	1.500 to 1.518	1.3795 to 1.3810
108 to 116	10.4	1.547	1.3799 to 1.3802

TABLE 2. *Decline of catalyst activity*

Cumulative feed	Feed rate	$C_6F_4HCF_3$ produced		Chloride production	
g	g/hr	Per g feed	Per hr	m eq/g	m eq/hr
34	22.7	0.136	3.1	0.94	21
102	34.5	---------	-------	.53	18
136	66.6	---------	-------	.25	17
211	33.6	.052	1.7	.39	13

3.5. Chloropentafluorobenzene Over Palladium

Chloropentafluorobenzene 9.6 g (0.0475 mole) and hydrogen (100 cm^3/min) were passed from the vaporizer at 98° to 102° C over 18 g of the palladium carbon catalyst packed in the middle section of the furnace tube, 17 cm by 2.5 cm, and maintained at 285° to 290° C. The wash waters contained chloride 0.064 equivalent (theory 0.047) and 0.008 equivalent fluoride. The product, 5.5 g, yielded the following fractions: (a) boiled at 88° to 91° C, 1.23 g, n_D^{20} 1.4051, possibly 1.2.4.5-tetrafluorobenzene and pentafluorobenzene; (b) boiled at 91° to 105° C, 1.00 g, n_D^{20} 1.4021, possibly 1,2,3,4-tetrafluorobenzene; (c) boiled at 105° to 112° C, 0.5 g, n_D^{20} 1.3990; (d) semisolid residue 2.7 g, n_D^{20} 1.3667.

3.6. Chloroheptafluorotoluene Over Palladium

2-Chloroheptafluorotoluene was passed over the palladium catalyst under the same conditions as above, but using a charge of 17 g (0.0675 mole) and a vaporizer temperature of 110° C. The time required was two hours. The wash waters yielded 0.075 equivalent chloride (theory 0.067) and 0.003 equivalent fluoride. The product contained α,α,α,3,4,5,6-heptafluorotoluene, $C_6F_4HCF_3$, boiled at 102° to 105.5° C, $n_D^{20.5}$ 1.3750, in a yield of 11 g (79.8%), and 1 g of residue.

3.7. Chlorotetrafluorobenzene Over Palladium and Nickel

1-Chloro-2,3,4,5-tetrafluorobenzene, boiled at 122° to 123° C, d_4^{24} 1.534, n_D^{24} 1.4407, was passed over nickel and palladium catalysts under conditions summarized in table 3. A typical experiment will be described elsewhere [5]. The conversion over nickel was relatively low, but conversion and yield over palladium were very high. A total of 1,020 g of feed were converted over a single charge of catalyst without noticeable change of activity. The purest fraction of product was 1,2,3,4-tetrafluorobenzene, boiled at 95° C, $d_4^{25.5}$ 1.4010, $n_D^{20.2}$ 1.4095.

TABLE 3. *Hydrogenation of C_6F_4ClH*

Charge weight	Catalyst	H_2 flow	Vaporizer temperature	Furnace temperature	Rate	Yield $C_6F_4H_2$	Halogen removed, equivalents per mole of feed	
							Cl^-	F^-
g		cm³/min	°C	°C	g/min	%	%	%
15	Ni powder	50	80	277	0.2	12	32	>1
123.5	20 g Pd, C[a]	100	108	280	.54	77.2	77	>1
92.4	do	100	108	280	.54	87.5	90.8	2.8
117.5	do	100	108	280	.54	84	77	>1
123.2	do	100	108	280	.54	78.2	73	>1

[a] ⅛ in. C pellets.

3.8. Hexafluorobenzene Over Palladium and Platinum

Hexafluorobenzene, C_6F_6, was passed over the palladium and platinum catalysts under conditions detailed in table 4. Runs are numbered in the order performed to illustrate cumulative effects. As the product was very incompletely separated by fractional distillation (table 5) the progress of reaction was routinely gauged by ionic fluoride liberated. The product from one run over palladium boiled at 82° to 86° C, had a refraction index $n_D^{2.65}$ 1.3870, and according to mass spectrographic analysis consisted of 45 percent C_6F_6, 40 percent C_6F_5H, 10 percent $C_6F_4H_2$, 4 percent $C_6F_3H_3$, and 1 percent $C_6F_2H_4$. A run preceding No. 1 showed no fluoride removed from C_6F_6 over palladium at 270° C, and one following No. 2 showed that the palladium catalyst had lost all its activity after that run at 325° C. The platinum catalyst declined much more slowly (runs 7 to 9). Catalyst activity had diminished to perhaps ⅔ of original activity after 950 g of feed had been processed. The platinum catalyst was inactive at 250° C and had an optimum temperature near 300° C (runs 5, 6, and 7). There was an initial period of lower activity (runs 3 and 4).

TABLE 4. *Hydrogenation of hexafluorobenzene* $C_6F_6 \xrightarrow{H_2} C_6F_5H$, $C_6F_4H_2$, $C_6F_3H_3$, etc.

Run	Charge weight	Time	Catalyst	H_2 flow	Vaporizer temperature	Furnace temperature	Weight recovered	F^- removed, equivalents per mole of feed
	g	*hr*		*cm³/min*	*° C*	*° C*	*g*	%
1	17.6	~2	Pd	100	~60	300	12.5	17
2	17.6	~2	do	100	~60	325	?	98
3	48	2.7	Pt	50 to 100	70	300	45	17
4	38.6	2.5	do	75 to 100	70	300	33	36
5	150	2.0	do	100 to 125	70	280	243	58
6	130	1.7	do	100 to 125	70	250		0
7	207	5.5	do	50	70	300		63
8	247	6	do	50	70	300	214	50
9	136	3.5	do	50 to 100	70	300	117	44

TABLE 5. *Products from* $C_6F_6 + H_2$

Boiling point ° C	80 to 82	82 to 84.5	84.5 to 90	>90
Specific gravity $d_4^{24.6}$	1.5273	1.5075	1.4336	1.3018
Refractive index n_D^{20}	1.3871	1.3910	1.4015	1.4112
Weight g	157	63	23	8
Mass spectrometric analysis:				
C_6F_6 mole %	73.2	Lost	22.2	6.8
C_6F_5H mole %	15.9	do	27.3	46.2
$C_6F_4H_2$ mole %	6.2	do	24.8	34.0
$C_6F_3H_3$ mole %	3.1	do	15.8	12.2
Lower F mole %	1.6	do	9.9	0.8

WASHINGTON, December 11, 1958.

4. References

[1] P. Sabatier and A. Mailhe, Compt. rend. **138,** 245 (1904).
[2] H. R. Arnold, and W. A. Lazier, U.S. Patent 2,025,032.
[3] F. Swarts, Acad. roy. Belg. Classe sci. [5]**6,** 399 (1920).
[4] N. V. Sidgwick, The Chemical Elements and Their Compounds, vol. 1, p. 122, Oxford, Clarendon Press, 1950.
[5] W. J. Pummer, R. E. Florin, and L. A. Wall, J. Research NBS **62,** (1959) RP2939.
[6] J. F. Burnnett and T. K. Brotherton, J. Am. Chem. Soc. **78,** 155 (1956).
[7] M. Hellmann, A. J. Bilbo, and W. J. Pummer, J. Am. Chem. Soc. **77,** 3650 (1955).
[8] E. Rinck, Bull. soc. chem. France **1948,** 305.
[9] E. T. McBee, V. V. Lindgren, and W. B. Ligett, Ind. Eng. Chem. **39,** 378 (1947).
[10] R. E. Florin, L. Wall, and W. J. Pummer, J. Research NBS **62,** (1959) RP2938.

Journal of Research of the National Bureau of Standards Vol. 62, No. 3, March 1959 Research Paper 2941

Exponential Integral $\int_1^\infty e^{-xt}t^{-n}dt$ for Large Values of n [1]

Walter Gautschi

An asymptotic expansion is given which is well suited for numerical computation when n is large and x arbitrary positive.

1. Let

$$E_n(x)=\int_1^\infty e^{-xt}\,t^{-n}dt; \qquad x>0; \qquad n=1, 2, 3, \ldots . \tag{1}$$

By means of four integrations by parts, G. Blanch[2] has found the approximation

$$E_n(x)\approx\frac{e^{-x}}{x+n}\left[1+\frac{n}{(x+n)^2}+\frac{n(n-2x)}{(x+n)^4}+\frac{n(6x^2-8nx+n^2)}{(x+n)^6}\right]. \tag{2}$$

She also gives an integral representation for the error. Formula (2) has proved very efficient for computing $E_n(x)$ for large values of n in the whole range $x>0$. In what follows, the complete expansion is given, as well as error estimates.

Denote by $h_k(u)$ the polynomial (of degree $k-1$ if $k>0$), defined recursively by

$$h_{k+1}(u)=(1-2ku)h_k(u)+u(1+u)h_k'(u) \quad (k=0, 1, 2, \ldots), \; h_0(u)=1. \tag{3}$$

Let

$$H_k(u)=\frac{h_k(u)}{(1+u)^{2k}}, \tag{4}$$

and let α_k, β_k be lower and upper bounds, respectively, for $H_k(u)$ in the interval $u\geq 0$:

$$\alpha_k\leq H_k(u)\leq\beta_k \qquad (u\geq 0). \tag{5}$$

Then it will be proved that

$$E_n(x)=\frac{e^{-x}}{x+n}\left[\sum_{s=0}^{k-1}H_s\left(\frac{x}{n}\right)n^{-s}+R_k(x,n)\right], \tag{6}$$

$$\alpha_k n^{-k}\leq R_k(x,n)\leq\beta_k\left(1+\frac{1}{x+n-1}\right)n^{-k}. \tag{7}$$

---

[1] This paper was prepared under a National Bureau of Standards contract with The American University.

[2] G. Blanch, An asymptotic expansion for $E_n(x)=\int_1^\infty (e^{-xu}/u^n)du$, NBS Applied Math. Series 37, 61 (1954).

For reference, the first eight polynomials $h_k(u)$ and corresponding values of α_k, β_k are listed:[3]

$$h_0(u)=h_1(u)=1$$

$$h_2(u)=1-2u$$

$$h_3(u)=1-8u+6u^2$$

$$h_4(u)=1-22u+58u^2-24u^3$$

$$h_5(u)=1-52u+328u^2-444u^3+120u^4$$

$$h_6(u)=1-114u+1452u^2-4400u^3+3708u^4-720u^5$$

$$h_7(u)=1-240u+5610u^2-32120u^3+58140u^4-33984u^5+5040u^6$$

$$\alpha_1=0, \quad \alpha_2=-0.07, \quad \alpha_3=-0.18, \quad \alpha_4=-0.36, \quad \alpha_5=-0.60, \quad \alpha_6=-0.94, \quad \alpha_7=-1.4$$

$$\beta_1=\beta_2=\beta_3=\beta_4=\beta_5=\beta_6=1, \quad \beta_7=1.8.$$

2. Consider, more generally, the integral

$$I=\int_a^b e^{f(t)}dt, \tag{8}$$

where $f(t)$ is a real function defined on the finite or infinite interval (a, b). It is assumed that $f(t)$ has derivatives of any order in (a, b) and that $f'(t)\neq 0$. Following van der Corput and Franklin,[4] we define the sequence $g_k(t)$ by

$$g_0(t)=\frac{1}{f'(t)}, \qquad g_{k+1}(t)=\frac{g_k'(t)}{f'(t)} \qquad (k=0,1,2, \ldots). \tag{9}$$

Setting

$$I_k=\int_a^b g_k(t)f'(t)e^{f(t)}dt,$$

clearly $I_0=I$, and integration by parts yields

$$I_k=[g_k(t)e^{f(t)}]_a^b-\int_a^b g_k'(t)e^{f(t)}dt=v_k-I_{k+1}, \tag{10}$$

where

$$v_k=g_k(b)e^{f(b)}-g_k(a)e^{f(a)}. \tag{11}$$

Hence,

$$I=v_0-v_1+v_2-v_3+ \ \ldots \ +(-1)^{k-1}v_{k-1}+(-1)^kI_k, \tag{12}$$

$$I_k=\int_a^b g_{k-1}'(t)e^{f(t)}dt. \tag{13}$$

---

[3] The author is indebted to Mrs. L. K. Cherwinski and Mrs. B. H. Walter for the calculation of the α_k and β_k.

[4] J. G. van der Corput and Joel Franklin, Approximation of integrals by integration by parts, Nederl. Akad. Wetensch. Proc. Ser. [A] 54 213-219 (1951).

In case of an infinite interval (a, b) it has to be assumed that the values (11) exist for all k. Equation (10) then shows that the existence of the integral I_k implies the existence of I_{k+1}.

3. The integral in (8) is equal to $E_n(x)$ if

$$f(t)=-(xt+n\ln t), \qquad a=1, \qquad b=\infty.$$

A short computation shows that with this definition of $f(t)$, the sequence $g_k(t)$ in (9) is equal to

$$g_k(t)=\frac{(-1)^{k+1}t}{xt+n}\,\frac{h_k(u)}{(1+u)^{2k}}\,n^{-k}=\frac{(-1)^{k+1}t}{xt+n}\,H_k(u)n^{-k}, \quad u=\frac{xt}{n},$$

where the $h_k(u)$ are the polynomials defined in (3) and $H_k(u)$ the rational functions (4). For the quantities v_k in (11), one obtains

$$v_k=\frac{(-1)^k e^{-x}}{x+n}\,H_k\left(\frac{x}{n}\right)n^{-k}.$$

Furthermore,

$$g'_{k-1}(t)=(-1)^k H_k(u)n^{-k}, \qquad u=\frac{xt}{n}.$$

Hence, from (12) and (13),

$$E_n(x)=\frac{e^{-x}}{x+n}\left[\sum_{\kappa=0}^{k-1}H_\kappa\left(\frac{x}{n}\right)n^{-\kappa}\right]+n^{-k}\int_1^\infty H_k\left(\frac{xt}{n}\right)e^{-xt}t^{-n}dt. \tag{14}$$

By (5)

$$\alpha_k E_n(x)\le\int_1^\infty H_k\left(\frac{xt}{n}\right)e^{-xt}t^{-n}dt\le\beta_k E_n(x),$$

and using the well-known inequality,[5]

$$\frac{1}{x+n}\le e^x E_n(x)\le\frac{1}{x+n-1} \qquad (x\ge 0),$$

one gets

$$\alpha_k\,\frac{e^{-x}}{x+n}\le\int_1^\infty H_k\left(\frac{xt}{n}\right)e^{-xt}t^{-n}dt\le\beta_k\,\frac{e^{-x}}{x+n-1}.$$

From this and (14) the formulas (6), (7) follow immediately.

It may be observed that the result (6), (7) holds also for nonintegral values of n with $n>1$.

---

[5] E. Hopf, Mathematical problems of radiative equilibrium, Cambridge Tracts in Mathematics and Mathematical Physics, No. 31, p. 26 (Cambridge University Press, 1934).

WASHINGTON, October 14, 1958.

Journal of Research of the National Bureau of Standards Vol. 62, No. 3, March 1959 Research Paper 2942

Effect of Oxygen on the Bonding of Gold to Fused Silica

D. G. Moore and H. R. Thornton

Gold pellets were melted on plaques of polished fused silica in vacuum and then heated for 15 minutes at 1,100° C under different oxygen pressures. The force required at room temperature to shear the solidified pellets from the silica surface was found to vary from zero for gold melted in vacuum to 725 pounds per square inch for gold melted under an oxygen pressure of 150 millimeters of mercury. In all cases where bond developed, fracture occurred in the silica rather than at the gold-silica interface. Silica plaques with pellets bonded to them by treatment in oxygen showed no measurable strain when examined with a polarograph, suggesting that the gold had yielded as the specimen cooled.

Tests using Au^{198} as a tracer indicated that gold diffused into the silica lattice at high oxygen pressure but that no diffusion occurred during vacuum heating. Observations made on molten droplets showed no correlation between the contact angles in air and vacuum and the apparent shear strengths. A possible explanation is included to account for this lack of agreement with theory.

1. Introduction

Recently, while investigating methods of bonding metals to ceramics, it was observed that a very strong bond developed when a small pellet of gold was melted on a fused silica surface in air. Because the gold gave a contact angle of approximately 140° (no appreciable wetting) and also, because there are no stable oxides reported for gold at its melting temperature, the observed bonding was believed worthy of further investigation.

The present paper summarizes the results of the more extensive study into this unexpected bonding behavior. The effect of oxygen pressure in the furnace atmosphere on bonding was determined; also, numerous observations were made on such effects as gold diffusion into silica, gas evolution, and residual strain. The various observations were then analyzed to determine their possible significance to bonding theory.

Earlier work on bonding in the Enameled Metals Laboratory was supported by the National Advisory Committee for Aeronautics. These earlier studies were mostly concerned with the adherence of vitreous coatings to metals [1–7].*

The present investigation was supported, in part, by the Bureau of Aeronautics, Department of Navy.

2. Materials

Three different golds were used in different parts of the program. Golds A and B were of similar purity. The identification of each of the gold samples and the results of their qualitative spectrochemical examination are given in table 1. No quantitative determinations were made.

The fused silica was procured as transparent optically-polished disks or plaques, ½ in. diam by ⅛ in. thick. A qualitative spectrochemical examination of a single disk showed that the principle metallic element impurities were aluminum and titanium which were estimated to be present in the range of 0.01 to 0.1 percent by weight. Other elements detected included silver, calcium, copper and magnesium estimated to be less than 0.001 percent, and manganese estimated to be less than 0.0001 percent.

*Figures in brackets indicate the literature references at the end of this paper.

TABLE 1. *Qualitative spectrographic analyses of golds* [a]

Metal	Description	Source	Impurities present in estimated concentration range of—		
			0.001 to 0.01 wt %	0.0001 to 0.001 wt %	<.001 wt %
Gold A	3-mm-diam high-purity rod.	(b)	None	Ag, Fe, Pb, Si	Cu, Ca, Mg
Gold B	Ingot prepared by melting purified sponge in graphite.	(c)	None	Cu, Ag, Fe, Pb, Si	Ca, Mg
Gold C	Metallurgically pure wire.	(d)	Ag, Si, Pd	Cu, Fe, Mg, Pb	Ca

[a] Analyses by Spectrochemistry Section; except for gold, elements other than those listed were not detected.
[b] Obtained from Johnson, Mathey and Co. Ltd., 73/83 Hatton Garden, London, England.
[c] Prepared at NBS.
[d] Source unknown.

3. Procedures and Results

3.1. Shear Strength Measurements

Gold B was obtained by melting gold sponge in vacuum in a high-purity graphite boat. After cooling, small pieces weighing approximately 0.5 g each were cut from the ingot with a sharp steel blade. The samples were immersed in warm hydrochloric acid for 15 min to remove contamination from the cutting operation.

The gold B specimens were next melted on the fused silica plaques in a small Nichrome-wound, Alundum tube furnace. The plaques rested on two sapphire rods which were leveled prior to test.

Two plaques were placed in the hot zone of the furnace for each test. The temperature was measured by means of a noble metal thermocouple, positioned adjacent to the plaques near the center of the furnace. The furnace was mounted in a large bell jar which could be evacuated to a pressure of 10^{-6} mm of mercury. The specimens were heated to 1,100° C in 20 min. During this heating period, the pressure in the bell jar never exceeded 6×10^{-4} mm of mercury. After 1 min at 1,100° C, oxygen that had been passed through a liquid nitrogen cold trap was admitted until the desired pressure had been reached. The temperature was then maintained at 1,100°±15° C for an additional 15 min after which the power was turned off and the specimens were allowed to cool with the furnace. The selected oxygen pressure was maintained throughout the 15 min heating period and also during the cooling. In the tests in which no oxygen was admitted, the pressure in the chamber was maintained at 3×10^{-5} mm during the 15 min heating period and also during cooling.

Air rather than oxygen was used for the furnace atmosphere in a few of the early tests. In these tests, the procedures were the same as when the tests were made in oxygen.

All gold pellets adhered to the silica surfaces except those heated in vacuum. Figure 1 shows a gold pellet on a fused silica plaque after the 15 min treatment at an oxygen pressure of 200 mm of Hg. Also shown is a similar specimen in which the gold pellet has been sheared from the silica surface. The surface of the silica glass has been shattered and slivers of silica are still adhering to the surface of the gold.

The equipment used for determining the force necessary to shear the gold pellet from the silica surface is shown schematically in figure 2. The silica plaque, with pellet attached, was first seated with a hard grade of plaster of Paris in the lower brass block (A) so that the top surface of the plaque was flush with upper surface of the brass. After the plaster hardened, a grease film was applied to the surface of the plaque, to the exposed surface of hardened plaster, and to the adjacent areas of polished brass. The upper brass block (B) was next centered over the specimen and the intervening space between the gold pellet and the hole in the upper block filled with plaster.

As soon as this second plaster investment hardened, the assembly was placed in position on the base plate (C) and a straight tensile force was applied to the upper brass block at the rate of 535 g per min. In each case the force required for failure was corrected for static friction. Several tests on a plaque with no gold shows this static friction varied between 85 and 110 g, the average being 98.5 g.

The area of contact between the gold and silica was determined by projecting a magnified image of the interface between the gold and silica on a ground glass screen. Thin paper was placed against the screen and a pencil trace made of the contact area. The paper was next cut along the traced lines and the weight of the cut-out area determined. This weight was then converted to area of contact from the known magnification and the previously determined weight per unit area of the paper.

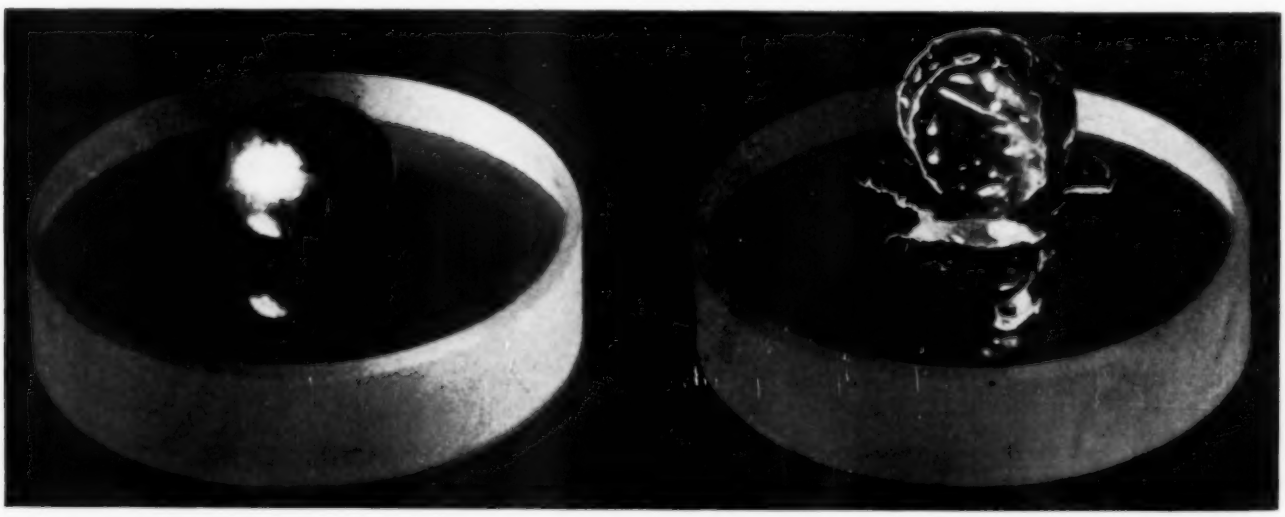

FIGURE 1. *Gold pellets on ½ in. diam fused silica plaques after 15 min heating at 1,100° C in oxygen at a pressure of 200 mm of Hg.*
Fracture occurred in glass rather than at interface when pellet at right was sheared from silica surface.

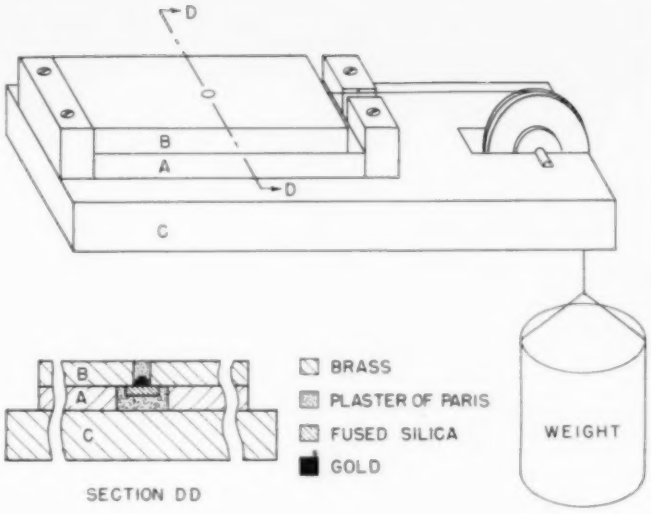

FIGURE 2. *Schematic drawing of shear test apparatus.*

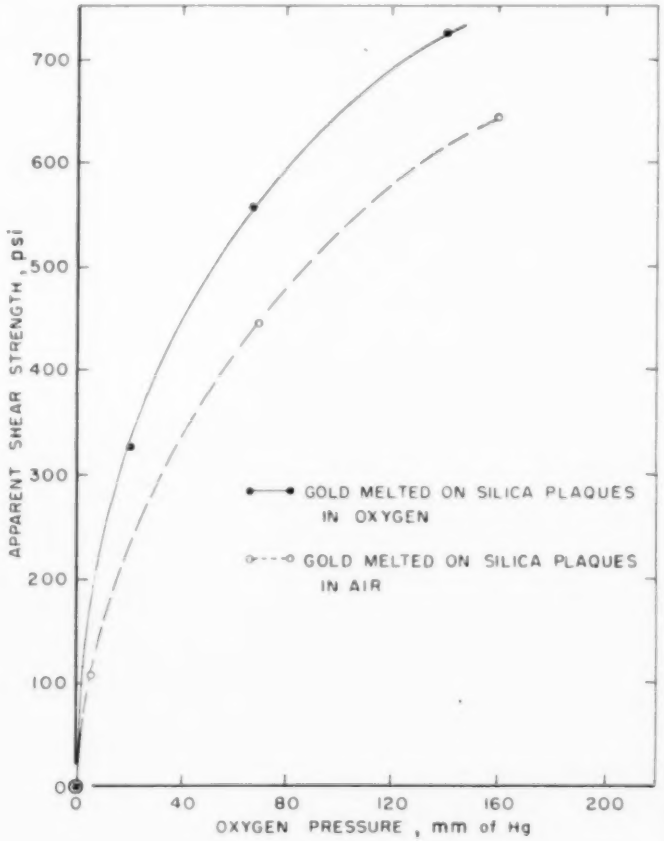

FIGURE 3. *Effect of oxygen pressure in the furnace on the room-temperature shear strength of gold pellets bonded to fused silica by heating 15 min at 1,100° C in air and oxygen.*

Shear strengths were obtained by dividing the force to cause fracture by the contact area; the values do not represent true bond strengths.

Figure 3 shows how the apparent shear strength changed with oxygen pressure when pellets of gold B were melted in air and in oxygen. The data used in plotting the two curves are listed in table 2. The value for the apparent shear strength at an oxygen pressure of 500 mm (spec. 13) is not plotted in figure 3. However, table 3 shows that it is lower than the value at 150 mm by some 15 percent, thus suggesting that the apparent shear strength may go through a reversal at high oxygen pressures.

TABLE 2. *Shear test results for 0.5 g pellets of gold B on fused silica plaques*

Spec. No.	Furnace atm.	Oxygen pressure in furnace	Shearing force for fracture	Contact area	Apparent shear strength	
		mm	*g*	*cm²*	*kg/cm²*	*lb/in.²*
1	Vacuum	0.6×10^{-6}	0	-------	0	0
2	do	0.6×10^{-6}	0	-------	0	0
3	Air	10	748	0.089	8.4	119
4	do	10	384	.052	7.4	105
5	do	65	2,460	.080	30.8	438
6	do	65	3,240	.102	31.7	451
7	do	152	2,990	.066	45.5	646
8	do	152	3,920	.088	44.4	631
9	Oxygen	18	2,420	.103	23.8	338
10	do	18	2,740	.126	21.7	308
11	do	65	2,350	.060	39.4	561
12	do	150	3,250	.064	50.8	722
13	do	500	3,480	.079	43.9	624

3.2. Observations of Strain in Fused Silica

The shear values plotted in figure 3 and listed in table 2 were measured at room temperature. During cooling the gold would contract at a much faster rate than the silica, thus tending to introduce strain into the system. To determine whether such strain was present, several silica disks were examined with a polarograph before pellets of gold A were sheared from the surfaces. The disks were viewed at several orientations, but in no case was any measurable strain detected. This condition could exist only if the gold yielded during the slow cooling in the furnace. Wrought and annealed high-purity gold is reported to have no yield strength (0.2% offset) at room temperature [8]; hence, such yielding is not unlikely.

The polarograph showed evidence of very slight strain in the silica for specimens with pellets of gold B and C, but this strain was too small for measurement with the polarograph.

3.3. Gas Occlusion at Interface

All specimens except those tested in vacuum showed gas occlusions present at the interface and, in some cases, the interfacial area taken up by the gas occlusions was as much as 50 percent of the total area of contact.[1]

[1] The area of observable voids was subtracted in determining the effective area of contact between gold and silica for computations of the apparent shear strengths.

An attempt was made to determine the stage in the melting and cooling operations at which the gas occlusions formed. A silica disk with a pellet of gold C at its midpoint was placed on a hollow refractory pedestal that projected up into the hot zone of a wire-wound tube furnace. A telescope having a magnification of 3x was then focused on the gold-silica contact area by sighting through the clear silica disk. A mirror placed immediately below the pedestal permitted the observations to be made with the telescope in a horizontal position. Differences in emissivity between the clear fused silica, the gold surface, and the gas occlusions gave good contrast at temperatures above about 800° C and no outside light source was needed.

The first observations were made in air. It was found that the gas occlusions began forming at the instant of melting and that they continued to grow in size for a period of several seconds. On further heating, the occlusions coalesced into several larger voids which remained substantially unchanged through several cycles of freezing and remelting. In other words, the observations in air were positive in showing that the entrapment of gas occurred only at the time of the first melting.

Similar experiments were made with the furnace placed in a vacuum chamber. The interface was observed through a window sealed into the bottom of the chamber. In these tests, no bubbles were observed on vacuum melting; however, tiny occlusions began to form at the interface shortly after air was admitted to the system and these grew slowly in size with continued heating at 1,100° C.

3.4. Etching of Silica by Gold

Pellets of gold A that had been melted on a silica plaque in vacuum and then heated for 15 min at 1,100° C at an oxygen pressure of 200 mm of Hg were dissolved from the silica surface with aqua regia. Examination of the silica surface after this treatment showed a very light etch at the outer edge of the gold-silica contact area. A similar etch also occurred at the outer edge of occluded gas bubbles. The etched surface on one of these fused silica disks was examined with the electron microscope. A replica was first prepared and this replica then shadowed by chromium vapor deposition prior to examination. Figure 4A shows the appearance that was typical near the outer edge of the contact area. The depth of these surface depressions is of the order of 30 mμ. Figure 4B shows an area of lesser attack while 4C is of a peculiar craterlike attack that was observed at one location near the gold-silica-oxygen interface. These craters extended into the silica to a depth of approximately 100 mμ.

As mentioned earlier, the gold pellets that had been melted and heated on silica plaques in vacuum came free of the silica surface on cooling. None of these plaques showed any evidence of a surface etch. Also, no etch was observed when one of these same plaques was immersed for 17 hr in aqua regia.

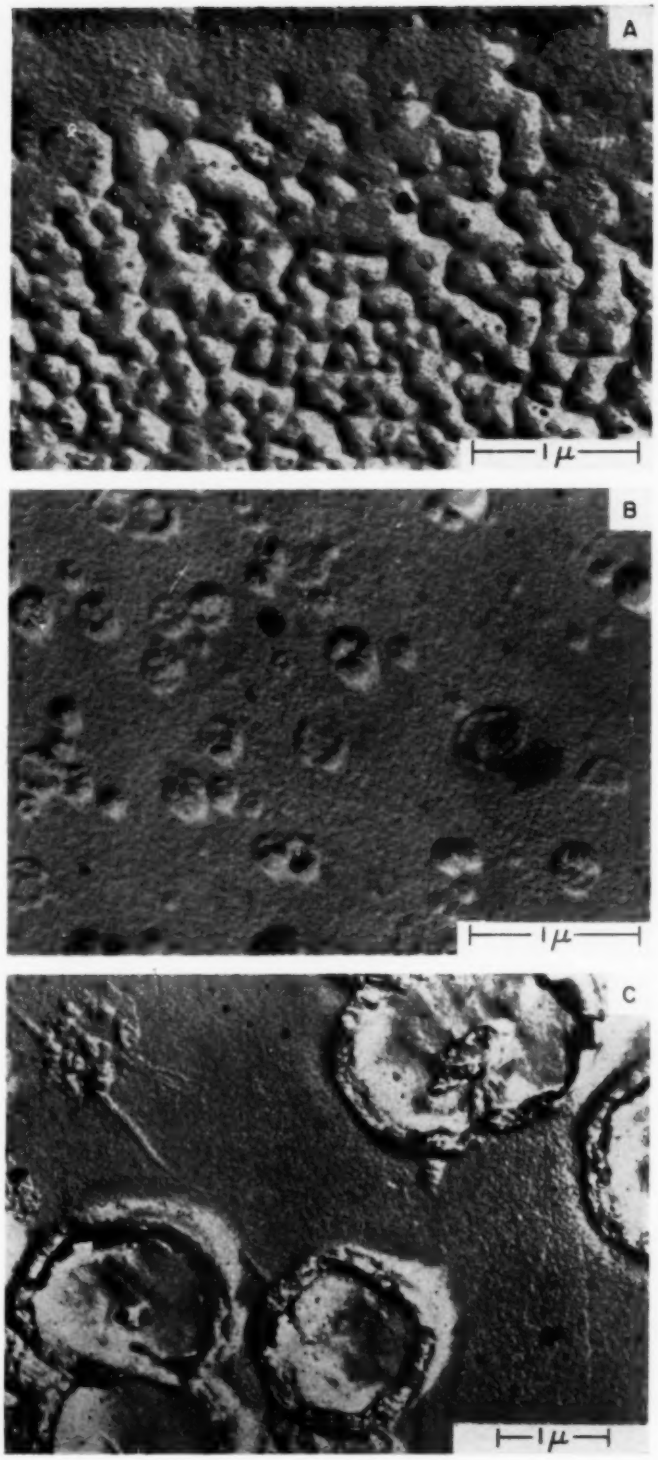

FIGURE 4. *Electron micrographs of the surface of fused silica from which the gold pellet had been dissolved with aqua regia.*

Specimen had been heated for 15 min at 1,100° C at an oxygen pressure of 200 mm of Hg. Micrographs are of replicas taken from "outer rim" of contact area.

3.5. Diffusion of Gold Into Silica

Two pellets of gold A were irradiated for 1 week in the graphite reactor at the Oak Ridge National

Laboratories. This treatment transformed some of the Au^{197} to Au^{198}. The Au^{198} isotope has beta emissions at 0.28, 0.96, and 1.37 Mev and gamma emissions at 0.41, 0.68, and 1.09 Mev. The half-life of the isotope is 2.7 days.

The first of the two pellets was placed on a silica plaque and heated to 1,100° C for 15 min in a vacuum of 3×10^{-5} mm Hg. On cooling, the pellet was lifted from the plaque and the plaque then immersed in aqua regia for 30 min to remove any vapor deposited gold from the silica surfaces (v.p. of gold at 1,100° C is approximately 10^{-5} mm of Hg). After thorough rinsing in water and drying, the plaque was placed in a lead shield with fixed geometry and a count made on the desired area with a scaler counter using a Geiger-Müller tube with a thin mica window. The count was not significantly above background, thus proving that no measurable diffusion of gold into silica had occurred during the vacuum melting operation.[2]

The second pellet also was melted on a silica plaque in vacuum but immediately after melting, oxygen at 200 mm pressure was admitted. The specimen was then heated at 1,100° C for 15 min in this atmosphere after which it was allowed to cool with the furnace. The pellet, which was firmly attached after cooling, was then dissolved from the silica plaque by placing the specimen in aqua regia at 24° C for 17 hr. Examination of the silica surface after removal of the gold showed that a light etching had occurred at the periphery of the contact area and also around occluded gas bubbles. The surface was radioactive. Counts were made on areas between small lead shields placed at selected locations on the plaque surface and these counts demonstrated that the activity was concentrated at the etched areas. This finding was later confirmed by an autoradiograph, an enlargement of which is shown in figure 5.

It is conceivable that the observed confinement of radioactivity to the etched areas could have been caused by gold chloride that had become adsorbed in these areas during the solution treatment in aqua regia. As a check on this possibility, the plaque was subjected to a series of treatments in boiling distilled water. Because gold chloride is soluble in hot water, such a treatment would be expected to remove at least a part of the dissolved salt. Counts were made before and after each treatment and these counts were compared with the normal decay rate of Au^{198} which was computed from the equation:

$$A=A_0e^{-0.693t/64.8} \quad (1)$$

where

A=activity at time t

A_0=activity at the beginning of the experiment

t=elasped time in hours.

The data, which are listed in table 3, show that no significant reduction in activity occurred from the boiling water treatments, thus indicating that the activity of the specimen was not caused by adsorbed gold chloride. It will be noted that the observed decay rate follows that for Au^{198} showing that the activity of the specimen was caused by Au^{198} and not by some trace impurity that was transformed to a radioactive isotope by treatment in the pile.

A second possibility was that the activity resulted from flecks of metallic gold that were not completely removed from the etched area by the 17-hr treatment in aqua regia. If this was the case, then treatment in warm aqua regia should reduce the activity of the specimen by a measurable amount. That such a reduction did in fact occur during the first of three treatments is shown by data listed in table 4.

These results suggest that a very small amount of gold was present either in the surface depressions or in the top layer of the silica lattice and that this gold was removed by the first half-hour treatment in warm aqua regia. However, the finding that further treatment caused no reduction beyond the normal decay rate, strongly indicated that some of the Au^{198} had diffused into the silica lattice. The actual amount was small, being of the order of 9×10^{-9} g, or 2.8×10^{13} atoms.[3]

FIGURE 5. *Autoradiograph (×10) of a surface of fused silica after removal with aqua regia of gold pellet containing* Au^{198}.

Region of Au^{198} activity corresponds with the outer edge of the contact area between the gold pellet and the silica. Specimen had been heated for 15 min at an oxygen pressure of 200 mm of Hg.

TABLE 3. *Effect of boiling water treatments on activity of silica plaque on which* Au^{198} *had been melted*

Time in boiling water	Elapsed time between counts	Activity in counts per min	
		Calculated from decay rate	Measured value [a]
hr	*hr*		
0	0	--------	225
0.25	1.0	223	218
2.0	3.5	217	215
16.0	21.0	180	182

[a] Average of five counts.

[2] It is possible that some gold may have been present in the outermost layers of the silica lattice and that this gold was dissolved by the aqua regia treatment. However, it is highly unlikely that gold which had diffused into the silica structure for a discrete distance could be removed by a relatively short treatment in aqua regia at room temperature.

[3] Computed from counts made from a gold standard prepared from foil that was irradiated in the same container with the pellets.

TABLE 4. *Effect of warm aqua regia treatments on activity of silica plaque on which* Au^{198} *had been melted*

Treatment in aqua regia		Elapsed time between counts	Activity in counts per min	
Time	Temp.		Calculated from decay rate	Measured value [a]
min	*° C*	*hr*		
		0		108
30	38	3	101	93
30	38	4¼	99	92
30	70	6¼	94	86

[a] Average of five counts.

3.6. Region of Maximum Bonding

Two experiments were performed in an attempt to determine if the observed bonding was concentrated in that region of the contact area where etching and gold diffusion had occurred; i.e., at the outer rim.

In the first experiment, silica plaques having different sized pellets of gold A positioned at their midpoint were prepared and treated for 15 min at 1,100° at an oxygen pressure of 10 mm of Hg. After cooling, the apparent shear strengths were measured. The results are listed in table 5. The trend of higher shear strengths with decreasing pellet size suggests that the bond was not uniform over the entire contact area, but rather that it was stronger along the outer rim.

TABLE 5. *Effect of size of gold pellet on apparent shear strength*

Weight of gold pellet	Au-SiO_2 contact area	Apparent shear stength	
g	*cm^2*	*g/cm^2*	*$lb/in.^2$*
0.129	0.0205	61,450	870
.556	.0565	56,900	810
.876	.0606	42,800	610

In the second experiment, four pellets of gold A, each weighing about 0.8 g, were placed on silica plaques and treated for 15 min at 1,100° C at an oxygen pressure of 100 mm of Hg. On cooling, the silica plaques were encased in a short section of brass tubing with plaster of Paris; the pellet in each case projected from the end of tube and was free of the plaster. The encased plaque was then placed in a lathe and the gold pellet machined down to about three-fourths of its original diameter. Individual cuts were of the order of 0.0005 to 0.001 in. During each pass, the lathe tool closely approached, but did not touch, the silica surface. The goal of the experiment was to compare the shear test values of normally prepared specimens with the values obtained on specimens from which the "outer rim" of gold had been removed.

The machining operation was attempted on all four specimens. In three of the specimens the gold came free of the silica before the diameter was reduced by the desired amount. Examination showed little or no fracture in the silica glass such as was invariably observed whenever oxygen-treated specimens with the "outer rim" intact were sheared from the silica surface (see fig. 1B). The machining of the fourth specimen was completed without separation of the gold pellet. However, the bonding was so weak with the "outer rim" removed that the pellet parted from the plaque when an attempt was made to mount the specimen in the brass block for the shear test determination. Examination showed no fracture in the silica surface.

Thus, although neither of the two experiments gave quantitative results, both indicated that the bonding was greater at the outer edge of the contact area than it was in the interior.

3.7. Contact Angle

A Leitz high-temperature microscope was used to observe and photograph molten drops of gold A(0.5 g) resting on polished plaques of fused silica. The furnace was platinum-wound and could be operated in either air or vacuum. The drop was observed through a Vycor window sealed into the furnace shell.

Figure 6A is a photograph of a molten drop of gold A in vacuum (1×10^{-3} mm of Hg) at 1,100° C. Figure 6B shows the same drop 5 min after air had been admitted to the system. Contact angles were measured on enlarged prints using a precision protractor. The angle in vacuum (fig. 6A) was 138°; the angle in air (fig. 6B) was 136°.

4. Discussion of Results

Release of strain by yielding of the gold during cooling permitted the apparent shear strengths to be measured at room temperature. Without this yielding excessive stresses would have been generated during cooling because of the large differences in thermal expansion coefficient (gold 16.9×10^{-6} per ° C from 20° to 1,000° C; fused silica about 0.6×10^{-6} over the same range). The polarograph was positive in showing that no strain was present for gold A on silica and no measurable strain for golds B and C. Even with no measurable strain, however, the shear test measurements did not give true bond strengths because of fracture in the silica glass. Also, if the bond is concentrated at the outer-rim of the contact area, as the experiments described in section 3.6 indicate, the shearing stress to cause failure of the bond would be much greater than the values listed in table 2.

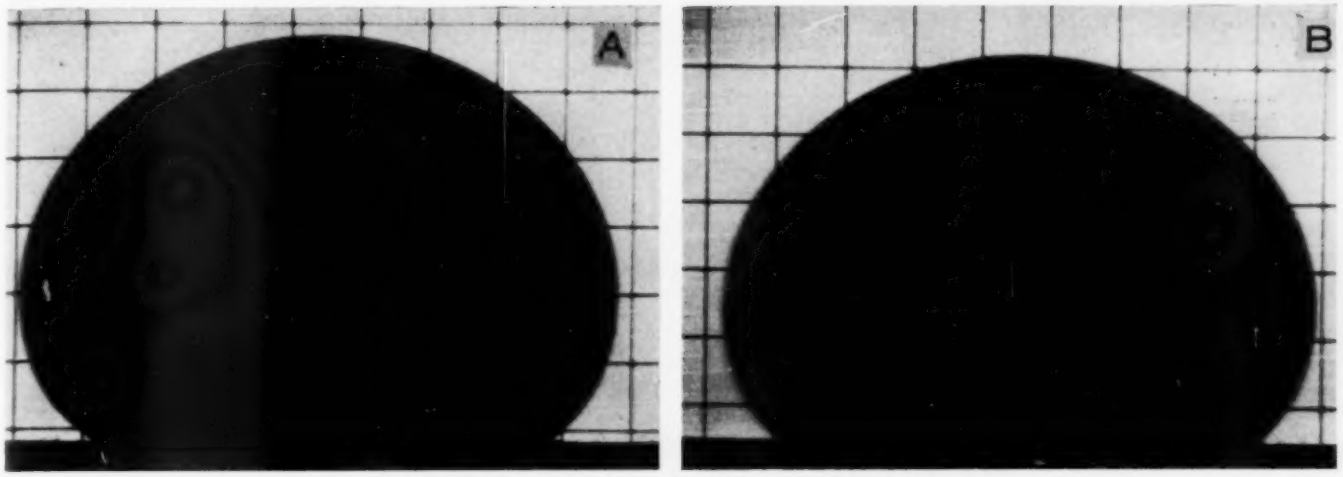

FIGURE 6. *Sessile drops of gold A on a silica plaque.*
A, In vacuum at 1,100° C; B, in air at 1,100° C. Sides of grid squares are 0.5 mm.

Impurities present in the fused silica undoubtedly had some influence on bond development but it is doubtful that the impurities exerted a controlling influence. A few tests made early in the study with high purity disks of polished sapphire gave the same type of results as were obtained with silica; the gold pellet developed no bond in vacuum yet in air the bond was so strong that fracture of the crystal occurred when the cooled pellet was pried loose from the sapphire surface. Baes and Kellogg [9] noted a similar behavior when working with sessile drops of copper that were cooled in contact with fused silica. In this system the presence of only a trace of oxygen permitted a strong bond to develop; fracture of the silica was observed when the pellet was pried from the surface.

Gas occlusions at the interface were noted for the specimens of gold melted on sapphire in air, as well as for specimens of gold on silica; gas occlusions were also noted by Baes and Kellogg [9] in the copper-silica system. The composition of the gas in the occlusions was not determined but is probably oxygen. According to Smithells [10], oxygen is strongly adsorbed by gold at room temperature. It may be that this adsorbed gas is released on melting and becomes trapped at the interface. Such a hypothesis, however, fails to explain why gold melted on silica in vacuum gradually accumulates occluded bubbles when air or oxygen is later admitted to the system.

Figure 4 shows that the silica surface in contact with the molten gold became slightly pitted during heating in oxygen. In the case of porcelain enamels on steel, Richmond et al. [2] showed that a correlation existed between roughness of interface and adherence. The etching of the steel occurred during the firing treatment. "Anchor points" were detected at the interface which could conceivably have caused a mechanical anchoring of the enamel layer. Later work by Moore and Eubanks [7] showed, however, that excellent bonding was possible without detectable interface roughening when similar enamels were applied to stainless steel. The pitting of the silica as observed in the present study was of a very small magnitude as is shown in figure 4. It seems highly unlikely that roughness on this scale could provide any appreciable mechanical interlock between the gold and silica.

All of the known oxides of gold decompose to the metal when heated at temperatures above 250° C. Recently, however, Carpenter and Maier [11] noted that oxygen was consumed when gold filaments were heated to about 900° C at oxygen pressures in the range ;1 to 10 μ. Their tentative explanation for the loss of oxygen was that a volatile gold oxide formed and deposited on the walls of the chamber. Finch and coworkers [12] observed extra rings in electron diffraction studies when gold foil was heated to 300° C in air. These rings, which corresponded to a close-packed hexagonal structure, disappeared when the foil was reheated in vacuum. They concluded that the oxygen entered the gold lattice, forming a solid solution within the surface layers.

Thus, there is some evidence for a gold-oxygen interaction at high temperatures and, in fact, such a reaction appears to be necessary to explain the strong bonds that were observed when oxygen was present. One possible explanation for bond formation in the presence of oxygen is as follows; (a) a relatively small amount of gold oxide forms by oxidation when the gold is heated to 1,100° C in the presence of oxygen, (b) some of the oxide that forms at the edge of the contact area between the gold droplet and the silica diffuses into the glass structure, and (c) a strong bond developes between the droplet and the gold-enriched layer of silica.

The formation of bond when the oxide of the substrate metal diffuses into a glass is in keeping with the results of a recent investigation by King and coworkers [13]. These investigators reported that strong "chemical bonds" developed only when a glass was "saturated" with the ion of the metal with which the glass was in contact. Such a requirement presupposes that there is a strong bond linkage between the atoms of the substrate metal and the ions of the same metal in the glass. Before accepting this hypothesis, it would need to be shown conclusively that an affinity of this kind actually exists.

In the foregoing it has been assumed that gold atoms could not enter the silica lattice structure and that for such diffusion to occur the gold would need to oxidize and enter the lattice as gold oxide. The observation that diffusion occurs only when oxygen is present supports this contention. Weyl [14], on the other hand, cites numerous examples from the German literature in support of small amounts of metal being soluble in glasses and molten salts. If such solubility can occur, and if metal solubility in the glass is enhanced by the presence of ions of the same metal, as implied by Weyl [14], then it is conceivable that a strong linkage might develop between the metal atoms dissolved in the outermost layers of the glass and the metal atoms in the substrate.

5. Comments on Lack of Correlation Between Contact Angle and Bond Strength

The observation that wide variations in bond occurred without any appreciable change in contact angle is contrary to what might be expected from surface energy relationships. For example, the work of adhesion, which is defined as the work required to separate a liquid from a solid, is given by the following expression:

$$W_{adh} = E(1+\cos\theta) \qquad (2)$$

E=surface energy between liquid and its vapor

θ=contact angle between liquid and solid when measured through the liquid.

When $\theta=0$ the liquid completely wets the solid and the work of adhesion is equal to twice the surface tension of the liquid. Because the degree of bonding should be related to work of adhesion, many investigators associate good bonding in a stress-free system with low contact angles and poor bond with high angles. The observations with the polarograph showed little or no stress in the system; hence, from eq (2), almost equal works of adhesion (similar bond strengths) would be predicted for the specimens heated in air ($\theta=136°$) and in vacuum ($\theta=138°$). The finding that the strength of the bond was different by many orders of magnitude suggests that either (1) the contact angle observed in air is not a true equilibrium angle, or (2) the energy relationships of eq (2) do not apply to this system.

Concerning the first possibility, it seemed conceivable that the contact angle observed in air might be dependent on the extent to which gold had diffused laterally along the silica surface. To test this possibility, an experiment was performed in which a pellet of gold A was first melted on a silica plaque in air. On cooling, the upper portion of the pellet was removed by hand filing, giving the shape shown in figure 7B. This was done carefully so as not to disturb the bond to the silica surface. The specimen was then remelted in air. Figure 7C shows that the new molten droplet did not pull away from the original line of contact but rather assumed a new shape with a smaller contact angle. This behavior at least suggests that once diffusion of gold ions has occurred the molten gold will then wet the silica. It also suggests that the contact angle observed during heating in air is not an equilibrium angle but rather might be expected to change with time as

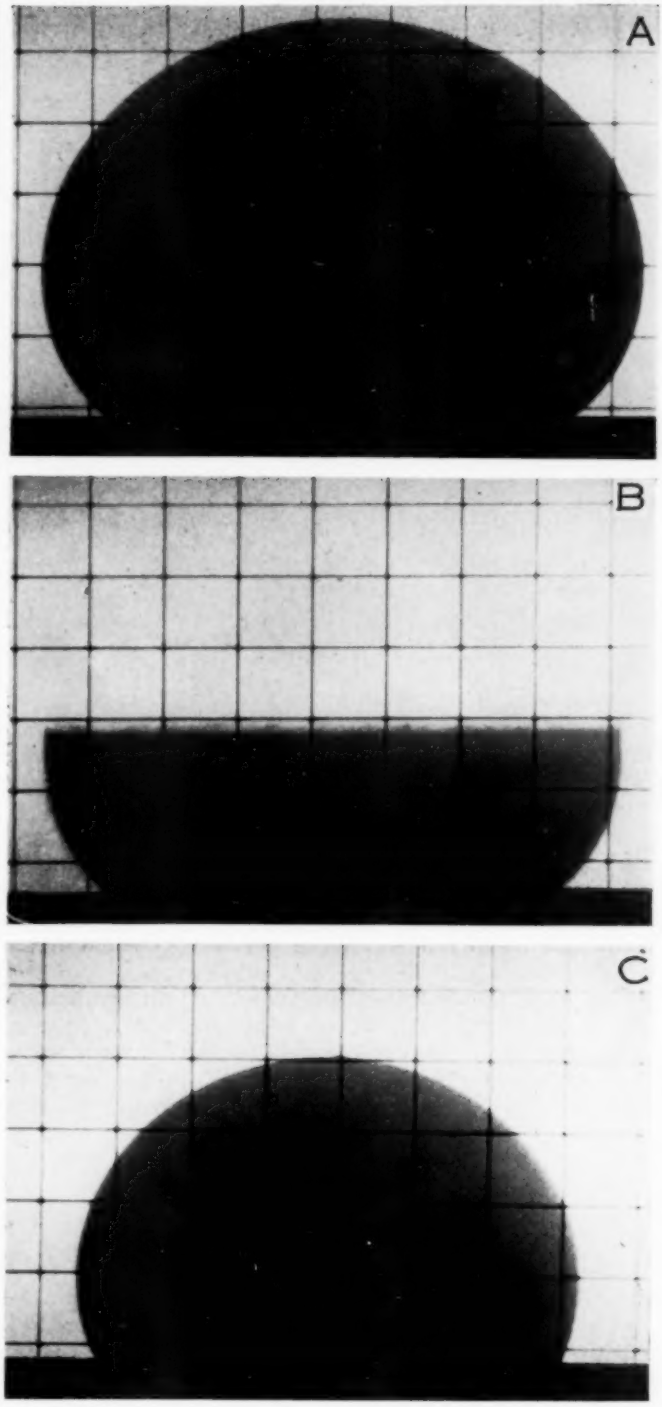

FIGURE 7. *Sessile drops of gold A on silica plaque.*

A, In air at 1,100° C; B, same drop at 20° C after removal of top portion by hand filing; and C, same pellet as B at 1,100° C in air. Sides of grid squares are 0.5 mm.

gold oxide diffused laterally along the surface of the silica.[3] Testing of this hypothesis by long-time heating, however, was impossible because prolonged heating at 1,100° C causes the silica glass to devitrify.

The second possibility, namely that the energy relations of eq 2 do not apply to this or to any real system, is not without some merit. Tabor [15] has pointed out two fundamental defects in the thermodynamic approach. The first is that the thermodynamic quantities connected with the work of adhesion are concerned with the energy change occurring when the liquid is placed on or removed from the surface. These quantities, however, tell nothing about the force with which the adsorbed film will resist shear in a direction tangential to the surface. The second is that in the formation of two new surfaces by rupture, by far the greater part of the energy in most real systems is dissipated in deforming either or both solids and the surface energy is only a small part of the whole energy involved. Yet a third factor is the large influence of stress concentrations along the periphery of the contact area between the adhesive and adherend. These stress concentrations appear whenever a shearing force is applied to a joint and their presence may completely mask any relationship between contact angle and work of adhesion. A discussion of the effects of stress concentrations has been given by de Bruyne [16].

In view of the foregoing considerations, the lack of correlation between work of adhesion and bond strength in the present experiment is not surprising. In fact, it seems unlikely that a correlation of this type would be observable in any real system.

The authors are indebted to Warren D. Hayes who photographed the droplets of molten gold also to W. N. Harrison, Chief of the Enameled Metals Section, for his many helpful suggestions.

[3] It is of course possible that the 22° decrease in contact angle as illustrated in figure 7 ($\theta = 137°$ in A and 115° in C) might be ascribed to the difference in angle that is sometimes observed when a liquid is (a) advancing or (b) receding over the surface of a solid. If this explanation is correct, then some change in contact area might logically be expected for the different sized drops (fig. 7A and 7C) but such a change was not observed.

6. References

[1] W. N. Harrison, J. C. Richmond, J. W. Pitts, and S. G. Brenner, Migration of cobalt during firing of ground coat enamels, NACA Tech. Note 2695 (1952); also, J. Am. Ceram. Soc. **35,** 305 (1953).

[2] J. C. Richmond, D. G. Moore, H. B. Kirkpatrick, and W. N. Harrison, Relation between roughness of interface and adherence of porcelain enamel to steel, NACA Tech. Note 2934 (1953); also, J. Am. Ceram. Soc. **36,** 410 (1953).

[3] D. G. Moore, J. W. Pitts, J. C. Richmond, and W. N. Harrison, The galvanic corrosion theory for adherence of porcelain enamel to steel, NACA Tech. Note 2935 (1953); also, J. Am. Ceram. Soc. **37,** 1 (1954).

[4] D. G. Moore, J. W. Pitts, and W. N. Harrison, Role of nickel dip in enameling of sheet steel, NACA Tech. Note 3207 (1954); also, J. Am. Ceram. Soc. **37,** 363 (1954).

[5] A. G. Eubanks and D. G. Moore, Effect of oxygen content of furance atmosphere on adherence of vitreous coatings to iron, NACA Tech. Note 3297 (1955); also J. Am. Ceram. Soc. **38,** 226 (1955).

[6] J. C. Richmond, H. B. Kirkpatrick, and W. N. Harrison, The nickel dip: a radioisotope study of metallic deposits in porcelain enameling, NACA Tech. Note 3577 (1956); also, J. Am. Ceram. Soc. **39,** 39 (1956).

[7] D. G. Moore and A. G. Eubanks, Influence of copper ions on adherence of vitreous coatings to stainless steel, NACA Tech. Note 3679 (1956); also, J. Am. Ceram. Soc. **39,** 357 (1956).

[8] Metals Handbook, p. 1117 (Am. Soc. Metals, Cleveland 3, Ohio, 1948).

[9] C. F. Baes, Jr. and H. H. Kellogg, Effect of dissolved sulphur on the surface tension of liquid copper, J. Metals **5,** 643 (1953).

[10] C. J. Smithells, Gases and Metals, p. 67 (Chapman and Hall, Ltd., London, England, 1938).

[11] L. G. Carpenter and W. N. Mair, Reaction between oxygen and hot gold, Nature **179,** 212 (1957).

[12] G. I. Finch, A. G. Quarrell, and H. Wilman. Electron diffration and surface structure. Trans. Faraday Soc. **31,** 1075 (1935).

[13] B. W. King, H. P. Tripp, and W. H. Duckworth, The nature of adherence of porcelain enamels to metals. (Presented at 58th Annual Meeting of Am. Ceram. Soc., New York City, 1956).

[14] W. A. Weyl, Colored glasses, 333–339 (Publ. by Soc. of Glass Tech., Northumberland Road, Sheffield 10, England, 1951).

[15] D. Tabor, Basic principles of adhesion, Repts. Progr. Appl. Chem. **36,** 621 (1951).

[16] N. A. de Bruyne, Fundamentals of adhesion, Research **6,** 362 (1953).

Washington, November 20, 1958

Important Notice

Beginning in July 1959, the Journal of Research will be published in four separate sections which may be subscribed for individually. This change is being made to provide a publication whose subject matter concentrates on particular fields of interest, thus meeting the specialized needs of individual scientists, engineers, and mathematicians.

Section A. Physics and Chemistry, to be issued bimonthly, will present papers of interest primarily to scientists working in these fields. This section will cover a broad range of physical and chemical research, with major emphasis on standards of physical measurement, fundamental constants, and properties of matter.

Section B. Mathematics and Mathematical Physics, to be issued quarterly, will present results in pure and applied mathematics, including mathematical statistics, theory of experiment design, numerical analysis, and short numerical tables; theoretical physics, chemistry, and engineering, where the emphasis is on the mathematical content or methodology; and logical design, programing, and applications of electronic computers and computer systems.

Section C. Engineering and Instrumentation, to be issued quarterly, will report results of interest chiefly to the engineer or applied scientist. This section will include many of the new developments in instrumentation resulting from the Bureau's work in physical measurement, data processing, and the development of test methods. It will also cover some of the work in acoustics, applied mechanics, building research, and cryogenic engineering.

Section D. Radio Propagation, to be issued bimonthly, will report research in radio propagation, communications, and upper atmospheric physics. Topics to be covered include propagation in ionized media, scattering by turbulence, the effect of irregular terrain on propagation, diffraction and scattering by solid obstacles, propagation through time-varying media, and antennas.

All present subscribers to the Journal will receive an announcement from the Superintendent of Documents when advance orders for the new sections can be accepted.

U. S. GOVERNMENT PRINTING OFFICE: 1959

THE NATIONAL BUREAU OF STANDARDS

The scope of activities of the National Bureau of Standards at its headquarters in Washington, D.C., and its major laboratories in Boulder, Colorado, is suggested in the following listing of the divisions and sections engaged in technical work. In general, each section carries out specialized research, development, and engineering in the field indicated by its title. A brief description of the activities, and of the resultant publications, appears on the inside front cover.

WASHINGTON, D.C.

Electricity and Electronics. Resistance and Reactance. Electron Devices. Electrical Instruments. Magnetic Measurements. Dielectrics. Engineering Electronics. Electronic Instrumentation. Electrochemistry.

Optics and Metrology. Photometry and Colorimetry. Optical Instruments. Photographic Technology. Length. Engineering Metrology.

Heat. Temperature Physics. Thermodynamics. Cryogenic Physics. Rheology. Engine Fuels. Free Radicals Research.

Atomic and Radiation Physics. Spectroscopy. Radiometry. Mass Spectrometry. Solid State Physics. Electron Physics. Atomic Physics. Neutron Physics. Radiation Theory. Radioactivity. X-rays. High Energy Radiation. Nucleonic Instrumentation. Radiological Equipment.

Chemistry. Organic Coatings. Surface Chemistry. Organic Chemistry. Analytical Chemistry. Inorganic Chemistry. Electrodeposition. Molecular Structure and Properties of Gases. Physical Chemistry. Thermochemistry. Spectrochemistry. Pure Substances.

Mechanics. Sound. Mechanical Instruments. Fluid Mechanics. Engineering Mechanics. Mass and Scale. Capacity, Density, and Fluid Meters. Combustion Controls.

Organic and Fibrous Materials. Rubber. Textiles. Paper. Leather. Testing and Specifications. Polymer Structure. Plastics. Dental Research.

Metallurgy. Thermal Metallurgy. Chemical Metallurgy. Mechanical Metallurgy. Corrosion. Metal Physics.

Mineral Products. Engineering Ceramics. Glass. Refractories. Enameled Metals. Concreting Materials. Constitution and Microstructure.

Building Technology. Structural Engineering. Fire Protection. Air Conditioning, Heating, and Refrigeration. Floor, Roof, and Wall Coverings. Codes and Safety Standards. Heat Transfer.

Applied Mathematics. Numerical Analysis. Computation. Statistical Engineering. Mathematical Physics.

Data Processing Systems. SEAC Engineering Group. Components and Techniques. Digital Circuitry. Digital Systems. Analog Systems. Application Engineering.

• Office of Basic Instrumentation.

• Office of Weights and Measures.

BOULDER, COLORADO

Cryogenic Engineering. Cryogenic Equipment. Cryogenic Processes. Properties of Materials. Gas Liquefaction.

Radio Propagation Physics. Upper Atmosphere Research. Ionospheric Research. Regular Propagation Services. Sun-Earth Relationships. VHF Research. Ionospheric Communications System.

Radio Propagation Engineering. Data Reduction Instrumentation. Modulation Systems. Navigation Systems. Radio Noise. Tropospheric Measurements. Tropospheric Analysis. Radio Systems Application Engineering. Radio-Meteorology.

Radio Standards. High Frequency Electrical Standards. Radio Broadcast Service. High Frequency Impedance Standards. Electronic Calibration Center. Microwave Physics. Microwave Circuit Standards.

Recent Publications of the National Bureau of Standards

Periodicals

Journal of Research of the National Bureau of Standards, volume 62, No. 1, January 1959 (RP2921 to 2928 incl.). 60 cents.

Technical News Bulletin, Volume 43, No. 1, January 1959. 15 cents. Annual subscription $1.50. 75 cents additional for foreign mailing.

Basic Radio Propagation Predictions for April 1959. Three months in advance. CRPL–D 173. Issued January 1959. 10 cents. Annual subscription $1.00. 50 cents additional for foreign mailing.

Circulars

C596. Single-phase transfer of liquefied gases. 30 cents.*
C600. Calibration of liquid-in-glass thermometers. 20 cents.*

Miscellaneous Publications

M225. Report of the 43d National Conference on Weights and Measures. 65 cents.*

Available from the Superintendent of Documents, U.S. Government Printing Office, Washington 25, D.C. The Technical News Bulletin and Basic Radio Propagation Predictions are available on a 1-, 2-, or 3-year subscription basis, although no reduction in rates can be made.

**Foreign postage, one-fourth additional.*

UNITED STATES
GOVERNMENT PRINTING OFFICE
DIVISION OF PUBLIC DOCUMENTS
WASHINGTON 25, D. C.

OFFICIAL BUSINESS

PENALTY FOR PRIVATE USE TO AVOID
PAYMENT OF POSTAGE, $300

Journal of Research of the National Bureau of Standards Vol. 62, No. 3 March 1959

Contents

		Page
On a theorem of M. Riesz. Martin Pearl.	RP2935	89
Refinement of the crystal structure of triclinic magnesium pyroborate. Stanley Block, Gorden Burley, Alvin Perloff, and Robert D. Mason, Jr.	RP2936	95
Heat transfer in laminar flow through a tube. Milton Abramowitz, William F. Cahill, and Clarence Wade, Jr.	RP2937	101
Fluorination of haloaromatic compounds. Roland E. Florin, Walter J. Pummer, and Leo A. Wall.	RP2938	107
Synthesis of some disubstituted 3,4,5,6-tetrafluorobenzenes. Walter J. Pummer, Roland E. Florin, and Leo A. Wall.	RP2939	113
Reactions of aromatic fluorocarbons with hydrogen. Roland E. Florin, Walter J. Pummer, and Leo A. Wall.	RP2940	119
Exponential integral $\int_1^\infty e^{-xt}t^{-n}dt$ for large values of n. Walter Gautschi.	RP2941	123
Effect of oxygen on the bonding of gold to fused silica. D. G. Moore and H. R. Thornton.	RP2942	127

[A list of recent NBS publications is given on page 3 of the cover.]

IMPORTANT NOTICE

Beginning in July 1959, the Journal of Research will be published in four separate sections. See the announcement given on the last page of this issue.

For sale by the Superintendent of Documents, U.S. Government Printing Office, Washington 25, D.C. Price 60 cents (single copy).
UNITED STATES GOVERNMENT PRINTING OFFICE, WASHINGTON : 1959